69-53

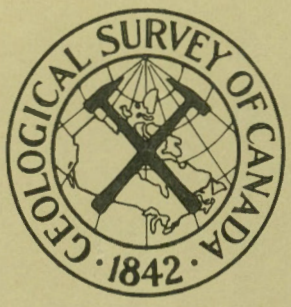

GEOLOGICAL
SURVEY
OF
CANADA

DEPARTMENT OF ENERGY,
MINES AND RESOURCES

PAPER 69-53

SERPENTINE MINERALOGY OF ULTRABASIC INTRUSIONS IN CANADA AND ON THE MID-ATLANTIC RIDGE

(Report, 10 figures and 11 tables)

F. Aumento

GEOLOGICAL SURVEY
OF CANADA

PAPER 69-53

SERPENTINE MINERALOGY OF ULTRABASIC INTRUSIONS IN CANADA AND ON THE MID-ATLANTIC RIDGE

F. Aumento

DEPARTMENT OF ENERGY, MINES AND RESOURCES

Available by mail from the Queen's Printer, Ottawa

from the Geological Survey of Canada
601 Booth St., Ottawa

and

Canadian Government bookshops in
HALIFAX - 1735 Barrington Street
MONTREAL - 1182 St. Catherine Street West
OTTAWA - Corner Mackenzie and Rideau
TORONTO - 221 Yonge Street
WINNIPEG - 499 Portage Avenue
VANCOUVER - 657 Granville Street
or through your bookseller

Price: $2.00 Catalogue No. M44-69-53

Price subject to change without notice

Queen's Printer for Canada
Ottawa
1970

CONTENTS

Illustrations

Page

Appendix

ABSTRACT

The serpentines and associated minerals from the stratiform Muskox Intrusion, the Alpine-type Mount Albert and Jeffrey (asbestos) Mine intrusions, and the Mid-Atlantic Ridge were investigated by X-ray diffraction techniques.

Lizardite is the predominant mineral formed in the serpentinization of both the ultramafic and mafic rocks of the Alpine, stratiform and mid-oceanic ridge intrusives. Lizardites from the Mid-Atlantic Ridge were found to have the smallest cell parameters, whereas the largest parameters occurred in the Alpine serpentinites. The latter were associated with abundant brucite, whereas in the Muskox and Mid-Atlantic Ridge serpentinites brucite was rare. The cell parameters and brucite content variations are indicative of different temperatures of serpentinization of the different intrusive bodies: the hottest temperatures (near 485° C) may have occurred on the Mid-Atlantic Ridge, intermediate to hot temperatures in the stratiform Muskox Intrusion, and the coolest temperatures (400° C or less) in the Alpine intrusives of Mount Albert and Jeffrey Mine. The latter are thought to have been serpentinized contemporaneously with the diapiric emplacement of cool, semicrystalline ultrabasic masses, whereas in the stratiform and mid-oceanic intrusives serpentinization probably occurred on cooling after emplacement and after termination of the processes of differentiation by crystal settling.

SERPENTINE MINERALOGY OF ULTRABASIC INTRUSIONS IN CANADA AND ON THE MID-ATLANTIC RIDGE

INTRODUCTION

The serpentine and related minerals from four chronologically, tectonically, and geographically distinct localities were selected for X-ray diffraction investigations to determine whether the serpentine minerals produced under different environments would show polymorphic variations as a result of any or all of the following variables:

(a) the difference between the alpine, stratiform and mid-oceanic ridge tectonic settings,
(b) the difference between the bulk chemical compositions of the original, preserpentinization, rock types (ultrabasic through to gabbroic),
(c) the chronological differences between the different environments (from Precambrian to Pliocene).

The serpentines for investigation were collected from the Muskox Intrusion, District of Mackenzie, Northwest Territories, a layered intrusion of Precambrian age; the Mount Albert Ultramafic Pluton, central Gaspé, Quebec, an Alpine-type intrusion of Ordovician age; the asbestos-producing Jeffrey Mine at Asbestos, Quebec, set in a differentiated ultrabasic intrusive sill of Ordovician age; and serpentinized ultrabasic rocks from the Mid-Atlantic Ridge at 45° N, of possible Pliocene age from a setting which is tectonically controversial and as yet not fully understood.

Review of Serpentine Mineralogy

The serpentine minerals are characterized by a common approximate composition of $H_4Mg_3Si_2O_9$, which is achieved by interlayering tetrahedral Si_2O_5 sheets and octahedral brucite sheets. Different serpentines are composed, however, of different arrangements of these two, basic, structural layers. Apical oxygens of the Si_2O_5 tetrahedra replace two out of every three hydroxyls on one side of the brucite layer only. The alternation of these layers of slightly different dimensions produces mismatching, which

---

Original manuscript submitted by author: 30 June, 1969
Final version approved for publication: 22 July, 1969
Project: 660041

causes strains within the sheets. In order that the structure remain stable this resultant strain must be compensated for.

The principal mechanism for strain relief in the layer alternations gives serpentines their characteristic morphology: curvature of the sheets occurs with the smaller tetrahedral components on the inside of the curves. This curvature is sufficient to produce bent crystals or tubes. Other strain-relief mechanisms include substitution of Si by larger ions to expand the tetrahedral sheets, or Mg by smaller ions to contract the octahedral sheets, or further physical distortion of octahedral and tetrahedral networks.

Similarities in chemical composition and structure make it difficult to distinguish between the various polymorphs. The factors favouring the formation of one polymorph rather than another are also not fully understood. The previous work on the serpentine minerals summarized below demonstrates the controversial and ambiguous nature of their mineralogy.

Previous X-ray Investigations

Selfridge (1936) provided the first reliable set of X-ray data for the serpentine minerals, together with chemical analyses of the samples and numerous thin section descriptions. On the basis of his findings, he attempted to condense the large number of names in use at that time for the serpentines into the following classification:

serpentine (massive rock)
chrysotile
antigorite
picrolite

Preferred orientations affecting the X-ray diffraction patterns, together with the different morphological aspects of the last two minerals listed, caused him to believe that antigorite and picrolite were two different minerals. The term "serpentine" for a mineral species is now considered meaningless, since it includes all the known polymorphs.

Although the structure of the fibrous serpentines had been suspected for some time, detailed investigation had been severely hampered by the lack of single crystals. Aruja (1945) was able to obtain single crystals of antigorite from Cropp River, New Zealand. He found a unit cell of dimensions $a = 43.39$, $b = 9.238$, $c = 7.265$ kX units with $\beta = 91.40°$. Systematic extinctions provided the choice of space groups C2/m, C2 or Cm. The single crystal photographs had the following characteristic features:

(1) there were streaks, and not sharp spots, parallel to the reciprocal 'c' axis when the index of 'k' was not a multiple of 3.

(2) superlattice effects gave variations in intensity of reflections in the reciprocal 'a' row line: spots were clustered in multiples of 8 about certain 'h' values, including zero. These could be explained by a subunit cell with $a = 5.42$, and a superlattice with $a = 43.4$ kX units.

(3) unexplained additional spots about the 'b' and 'c' axes (his material may not have been a single crystal).

(4) no Laue spots, but streaks only. These were assumed to be due to a packing error between sheets in steps of $b/3$ or $ma/2 + nb/6$ where n, m, are integers and $n + m$ = even. This insures noncoherent scattering when 'k' is a multiple of 3 (or $3h + k$ is a multiple of 6).

Aruja noticed a strong analogy between the intensities of antigorite patterns and those of chrysotile, especially as regards the (00ℓ) and 0k0 reflections. He suggested that antigorite has the same sequence of atomic planes parallel to (00ℓ) as in chrysotile, built up of kaolinite-like sheets with Mg substitution, giving O_6-Si_4-$O_4(OH)_2$-$Mg_6(OH)_6$ and repeats. Such a layer would be 7.3 kX units thick. On the basis of a few, very weak (20ℓ) reflections, he suggested a 'c' axis of 14.6 kX for chrysotile.

Further work on antigorite by Hess et al. (1952) included chemical, optical and differential thermal analyses. They arrived at the chemical formula: $Mg_7Si_5O_{13}(OH)_8 . n H_2O$ with 'n' values ranging from 1 to 3. They also concluded from field evidence that dynamothermal conditions (slightly higher than the chlorite-biotite subfacies of the granulite facies) could change chrysotile into antigorite; in the process chromite and magnetite would be gradually resorbed, leaving a pure antigorite rock.

Brindley and Von Knorring (1954) reported a new variety of antigorite from Unst, Shetland Islands. The X-ray data could be indexed on an ortho-hexagonal unit cell, with a = 5.322 Å, b = 9.219 Å, c = 2 x 7.265 Å; the mineral was named ortho-antigorite. The space group was given as $C6_3cm$. A closely spaced series of faint lines proceeding from the position (020) (from 4.6 to 2.7 Å), similar to the lines found in antigorite, suggested superlattice of S = 43.8 Å. D. T. A. curves were found to be similar to those for antigorite.

Zussman and Brindley (1957) verified that the superlattice was along the 'c' axis, and not along the 'a' axis, using electron diffraction investigations. The close approximation of this 6-layer cell to a 2-layer cell (for hkℓ reflections, ℓ = 3n is more intense than ℓ = 3n + 1) resulted in a further subdivision of the 6-layer ortho-hexagonal serpentines into 6 (2), as for ortho-antigorite, and 6 (3) for cells approximating to 3-layer systems. Another example of the 6 (2) 6-layer serpentines was recorded by Olsen (1961) from the Labrador Trough. Olsen noted variations in the spacings of (0kℓ) reflections between the Unst sample and the Labrador Trough sample, and attributed them to differences in composition.

Zussman (1954) suggested that the structure for antigorite postulated by Aruja (1945) was oversimplified. He visualized a curved and corrugated sheet-structure, with corrugations represented either by a rectified wave shape, or an alternating wave, or even a zig-zag structure.

A new mineral from Kennack Cove, Lizard, Cornwall, was reported by Midgley (1951), and was later called lizardite. D. T. A., chemical analyses, and diffraction patterns suggested that it was a new serpentine polymorph. The cell parameters were calculated to be a = 5.29, b = 9.18, c = 7.45 kX, with $\beta = 91.4°$, and a possible space group Cm, C2, or C2/m.

A number of serpentines from Glen Urquhart, Inverness-shire, Scotland were studied by Francis (1956). He gave diffractograms, forms, and optic orientations of the serpentines, on the assumption of curvature superimposed on a platy crystal.

With the assistance of single crystal rotation data, Whittaker (1956a, b, c) was able to distinguish three different polymorphs of chrysotile, namely clino-, ortho-, and para-chrysotile. Clino-chrysotile is based on a kaolin-like layer stacked to form a cylindrical helical structure of space group C2, with a = 14.65, b = 9.25, c = 5.34 Å and $\beta = 93° 16' \pm 1'$. Very weak reflections on layer lines, equal to fibre axes repeats of 9.24 Å are due to the presence of para-chrysotile, whilst very weak reflections near the

centre of the second layer line are the strongest spots (202) for ortho-chrysotile. Ortho-chrysotile is orthorhombic with a = 14.63, b = 9.2, c = 5.34 Å, and is always in intimate admixture with clino-chrysotile. The individual layers of the two minerals are almost identical, whilst the alternate layers are inverted end to end, leading to different stacking arrangements. Whittaker noted that specimens from Quebec are usually poor in their ortho-chrysotile content. Para-chrysotile is even rarer, forming at the most 3 per cent of a chrysotile specimen. The latter is orthorhombic cylindrical with a = 14.7 ± 0.1, b = 9.24 ± 0.02, c = 5.3 ± 0.1 Å, differing from the other chrysotile polymorphs in that the 'b' axis is parallel to the fibre axis.

In the light of the new information, Whittaker and Zussman (1956) classified the serpentines as follows:

chrysotile: ortho-
clino-
para-

lizardite
antigorite

They provide the most comprehensive powder and single crystal data to date. Para-chrysotile could only be detected in single-crystal photographs, whilst an attempt was made to detect admixtures of orthoclino-chrysotile in powder photographs. The ratio ortho/clino could best be determined by examining the zero and second layer line reflections on single crystal photographs. In those, and in powder photographs, (20ℓ) reflections have ℓ = odd stronger than ℓ = even for ortho-chrysotile, whilst ℓ = even is nonexistent for clino-chrysotile. However, ℓ = even is stronger than ℓ = odd for (20ℓ) reflections of lizardite. The determination of polymorphs, and especially of mixtures, is therefore highly dependent on careful intensity measurements.

Nagy and Faust (1956) claimed they were able to detect mixtures of chrysotile and antigorite by D. T. A. The latter were described in detail, together with a graph for the calculation of percentage antigorite in chrysotile by the examination of the (00ℓ) intensities in the X-ray diffractograms.

Gillery (1959), during a study of the synthesis of serpentines, produced a 6-layer cell serpentine similar to the natural 6(2) ortho-antigorite of Brindley and Von Knorring (op. cit.). However, this synthetic polymorph approximates a 3-layer cell, with ℓ=2n more intense than ℓ=2n+1 for hkl reflections, and is designated 6(3).

The crystal structure of lizardite was finally solved by Rucklidge and Zussman (1965). They gave it the ortho-hexagonal one-layer cell of a = 5.31 b = 9.2 and c = 7.31 Å, with a trigonal symmetry (verified by examination of systematic extinctions). They reported that although the layers are the same as those for chrysotile, significant differences are that:

(1) crystals are macroscopically bent about more than one axis.
(2) some layers are displaced by b/3.
(3) some layers are rotated through 180°

Aumento (1967) described an unstable serpentine polymorph which exhibits the combined properties characteristic of a number of other known polymorphs. Macrocrystals of the mineral, from the Tilly Foster Mine, New York State, indicate that it is a six-layered monoclinic serpentine, with each successive layer displaced relative to its neighbours by ± a/3, and ± b/3 and/or by a rotation of ± 60°. Individual layers are further modulated periodically in the a crystal direction. The resulting crystal has superlattice controlled a and c parameters. Finer fractions of a powdered macrocrystal,

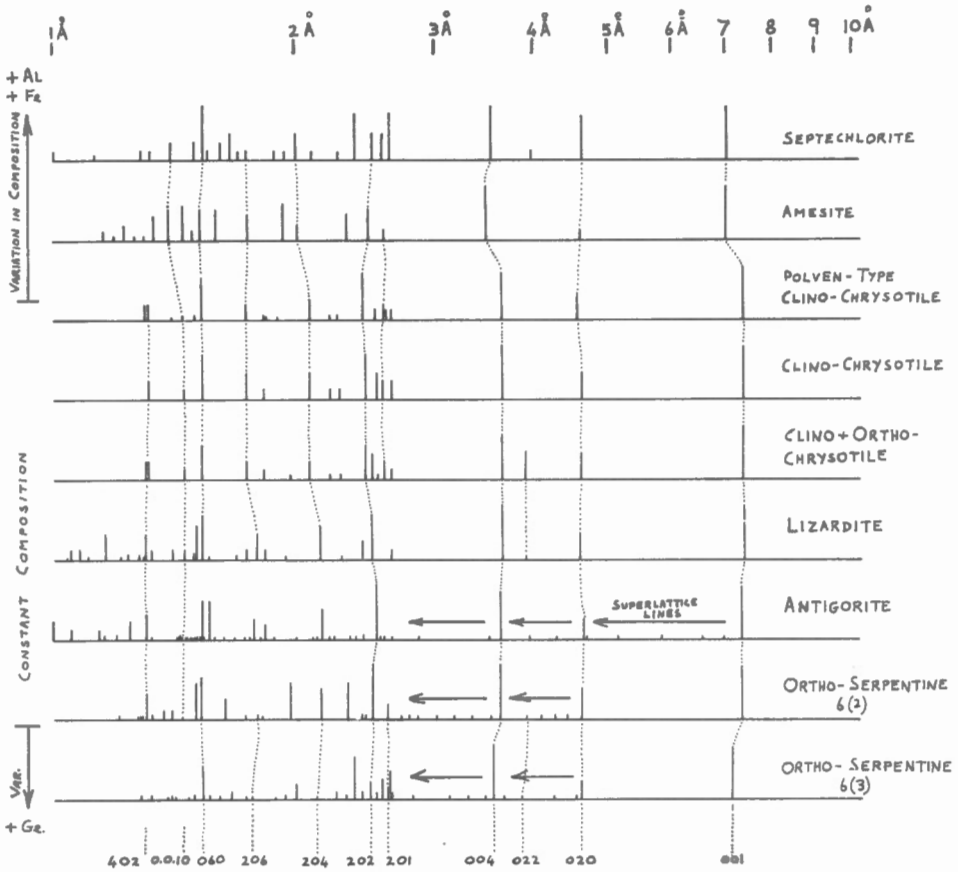

Figure 1. Schematic X-ray powder data for the serpentine polymorphs and minerals with similar crystal structures (amesite and septechlorite).

observed by electron microscopy, show that it tends to break down into smaller, simpler units; thin corrugated plates are formed, which themselves part along weak corrugation joints, forming elongated rods. The formation of rods deprives the basic serpentine layers of the satisfactory strain relief mechanism attributed to corrugation. The rods compensate for this deprivation by curling parallel to their elongation, eventually producing more stable chrysotile-like tubes. Aumento was able to follow the complete metamorphosis from plates to tubes by selected area electron diffraction.

The review of the latest literature led the author to modify the classification of the serpentine minerals of Whittaker and Zussman (1956). The new classification is based on additional structural characteristics, and includes all known polymorphs, at the same time eliminating the many unacceptable pseudonyms which have appeared through the years. The classification is as follows:

chrysotile:	clino-
	ortho-
	para-
lizardite:	natural
	synthetic one-layer ortho-serpentine.
antigorite:	massive and fibrous (picrolite)
6-layer ortho-serpentine:	6(2) ortho-antigorite.
	6(2) synthetic MgGe serpentine.
	6(3) synthetic Mg serpentine.
tilly serpentine	
septechlorite	Closely related minerals of structure similar to that of the serpentines, but of different chemical composition.
amesite	

Schematic X-ray powder data for the polymorphs listed above is presented in Figure 1. It will be noted that some of the patterns are suffering from strong preferential orientation, whilst many of the others are very similar. Assuming the data to be reliable, then distinctions rely more on observations of relative intensities between selected sets of diffraction peaks rather than on their angular positions.

D. T. A. and T. G. A.

Wide variations exist in recorded D. T. A. curves for similar polymorphs. Antigorite from Caracas, Venezuela (Hess, et al., 1952) gives two endothermic peaks only, a minor broad one at 120°C, and a major one at 782° C. Antigorite studied by Nagy and Faust (1956) does not give the first endothermic peak, but shows an additional one at 872° C. Antigorite from the Transvaal (Vermaas, 1953) gives a large endothermic peak at 760-778° C, followed by a large exothermic peak at 810-820° C. The latter curve is very close to one for chrysotile, which Vermaas shows to have a minor endothermic peak at 590-600° C, followed by a major one at 670-750° C, and a very sharp exothermic peak at 805-810° C. However, Nagy and Faust (op. cit.) find that chrysotile gives two minor exothermic peaks at 292 and 433° C, with a major one at 824° C, and a large endothermic peak at 710° C.

The only D. T. A. curve published for lizardite (Midgley, 1951) shows a diffuse endothermic peak at 100° C, a large double one at 650-700° C, and a sharp exothermic peak at 820° C.

The wide variations in D. T. A. data are interesting, as they have been shown to be due to other factors than simple instrumental effects. Naumann and Dresher (1966) have shown that sample texture, or microporosity, has a pronounced influence on chrysotile dehydroxylation at high temperatures.

Kalousek and Muttart (1957) noted a small but real difference in the binding strength of water between fibres and matrix (massive) serpentines. Thermo-gravimetric analyses showed two-stage dehydrations for the matrix, as opposed to a single one for the fibres. The second matrix dehydration occurs at a higher temperature than is required for brucite layers. No explanation is offered for this phenomenon, except that there may be extra tetrahedral 'water' in the matrix. Wolochow and White (1941) carried out

similar experiments on the effect of temperature and time on the loss in weight of chrysotile, but did not report any difference between fibres and matrix dehydration characteristics.

Electron Microscopy

Electron microscopy and diffraction techniques are ideally suited to the study of serpentine minerals. Not only can tubular, platy and amorphous morphologies (and their submicroscopic mixtures) be viewed, but also direct unambiguous identifications of the components can be made from observations of electron diffraction patterns.

Nagy and Faust (1956) noted an immediate difference between chrysotile and antigorite when exposed to the electron beam: the latter was quite stable, whereas the former disintegrated in a few minutes at high accelerating voltages.

More sophisticated distinctions are possible: Zussman et al. (1957) were able to formulate a serpentine classification on the basis of hand specimen morphologies versus dispersed state morphology as viewed under the electron microscope:

	Chrysotile	Lizardite	6-layer serpentine		Antigorite	
Hand specimen	fibrous massive	massive platy	massive fibrous	platy	massive platy	fibrous
Microscopic	tubes laths	plates	laths	plates	plates	broad laths

They were also able to make immediate identifications of the polymorphs by viewing the electron diffraction patterns. Chrysotile could be subdivided further into the ortho- and clino- varieties.

Whittaker (1956d) observed the chrysotile tubes from random ground dispersed fibre mounts. He noted that fibrils most commonly have internal and external diameters of 110 Å and 260 Å with 10 layers in tube walls. The strain-free radius is 88 Å. He was also able to reconcile the density evidence of hand specimens with electron microscope observations on the assumption that (1) interfibrillar voids are filled by layers in the form of cylindrical arcs coaxial with adjacent fibres; (2) intrafibrillar voids are filled as above, oriented parallel to, but not coaxial with, walls of fibres; (3) small proportions of fibres are hollow.

Huggins and Shell (1965) also suggest that more than 50 per cent of the tubes are hollow, whilst some are filled with water.

Improved views across fibres were obtained by Maser et al. (1960) by embedding fibres in resin and cutting from them oriented slices (ultramicrotomes) using a diamond knife. This technique has proved to be very successful, and also allows oriented electron-diffractograms to be made at will.

Electron optical fringes were obtained from antigorite (Yu Yen Stone) by Brindley et al. (1958). These fringes agree in spacings and direction with a superlattice parameter of a = 100 $\pm$ 10 Å which shows up in X-ray and

electron diffraction photographs. Chapman and Zussman (1959) demonstrated the existence of considerable variability in superlattice periodicity in crystals of antigorite even within the same crystal. With decreasing super-cell parameters, as in picrolite compared to antigorite, the small cell with a = 5.3 Å loses its significance in the structure. This is reflected in the less obvious clustering of spots in electron diffraction patterns. The variation detected is as follows:

Superlattice spacing	Occurrence	Locality
16 - 19 Å	picrolite	Taberg
35 - 45 Å	antigorite	Antigorio and Yu Yen Stone
80 - 110 Å	antigorite	Yu Yen Stone

Yada (1967) presented final visual proof of the cylindrical, multi-spiral structure of chrysotile by observing microfibres of chrysotile asbestos with a high resolution electron microscope (image resolution around 2 Å). He showed that most fibres have a hollow, cylindrical form, whereas others are not hollow, but solid, showing unusual growth patterns. His diffraction patterns suggest that the value of the 'c' parameter is 7.3 Å rather than 14.6 Å.

Chemical Analyses

In the past, chemical analyses have been unable to detect reliable differences between the different polymorphs, although certain researchers have noted inconclusively that variations do occur. Kalousek and Muttart (1957) noted that fibres have lower concentrations of Al_2O_3, Fe_2O_3 and FeO than the matrix. In fibres, the only extraneous substituent in the silica layer is tetrahedral water $(H^+)_4$ for (Si^4). They also noted that there are significant differences in ratios of intensities of diffraction lines at 7.3 and 3.6 Å with respect to total number of moles of Al^{3+}, Fe^{3+}, and Fe^{2+}. These ratios are higher for matrix material than for fibre material of the same composition. Bates (1959) found chemical differences between a number of platy serpentines and chrysotile, especially in the latter's lower SiO_2 content. Olsen (1963) noted that differences in composition possibly caused the differences in (0kℓ) spacings between different ortho-serpentines (ortho-antigorites 6 (2)). Soboleff and Tatarinoff (1933) attributed differences between normal, harsh and brittle chrysotile asbestos to water, SiO_2 and occasionally MgO content.

Over 200 serpentine analyses, plotted on triangular diagrams by the author, show diffuse composition fields for the different polymorphs (Fig. 2). However, the chemical differences are so small that only classical chemical analyses can be used to distinguish the polymorph fields; this automatically excludes the possibility of a large-scale analytical approach to the serpentine study. In addition, analytical data are always suspect, due to the impossibility of controlling the purity of the specimen concentrates to be analyzed.

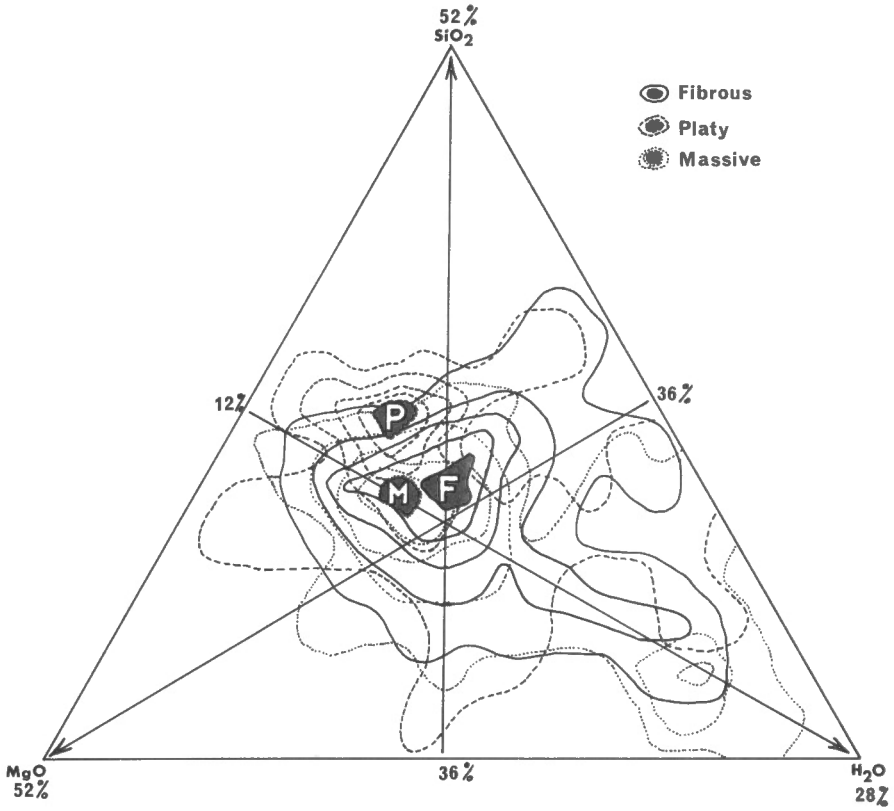

Figure 2. Triangular diagram plot of SiO_2, MgO and H_2O content of fibrous (the chrysotiles), platy (antigorites, ortho-serpentines) and massive (mainly lizardites) serpentines, arbitrarily contoured to indicate relative distribution fields.

Optical Investigations

Previous work has shown that at the most, refractive indices can distinguish between the chrysotile polymorphs, lizardite, and antigorite. Microscopy is therefore limited to preliminary thin section determinations, and as an aid to the selection of material for further investigations.

Thermal Transformations

A study of the thermal transformations, heating and dehydration characteristics of the different polymorphs has already shown strong .

possibilities of correlation of these characteristics to the structure types. However, opinions differ as to the exact type and sequence of events.

Aruja (1945) noted a gradual change in the diffractograms of chrysotile at 750° C, when, after 20 hours of annealing, the pattern was completely replaced by forsterite (a weak enstatite line was sometimes detected also). Epprecht and Brandenburger (1946) noted a modification on the chrysotile phase at 530° C, followed by gradual replacement by forsterite at 560° C (complete at 650° C) and an incipient appearance of enstatite at 1100° C. Hargreaves and Taylor (1946), however, found no change in chrysotile until 600° C, when different amounts of forsterite were formed in different samples of chrysotile. In one case a completely semiamorphous pattern was obtained at 600° C.

Hey and Bannister (1948) also obtained forsterite, water + silica + gel on heating chrysotile, but they suggested the presence of an additional amorphous phase ($Mg_3Si_2O_9$) below 1000° C. Vermaas (1953) detected forsterite between 810° C and 1890° C (its melting point), with the addition of small amounts of enstatite in the range 1000° C to 1400° C only.

Brindley and Zussman (1957) carried out a more comprehensive study of the thermal transformation of silky chrysotile, splintery chrysotile, antigorite, lizardite and 6-layer ortho-serpentines. Transformations appeared to be the same for all the polymorphs, except that those for silky chrysotile tended to occur at slightly lower temperatures than those of the others. Platy antigorite required the highest temperatures. Studies on single-crystal thermal transformations, on the other hand, showed different orientations of the new phases depending on the starting material.

Synthesis

Bowen and Tuttle (1949), in the study of the system $MgO\text{-}SiO_2\text{-}H_2O$, arrived at experimental data for the formation and survival of serpentines which has since been strongly disputed by field geologists. They concluded that chrysotile can only be prepared at temperatures below 500° C $\pm$ 10° C at pressures from 20,000 to 40,000 psi, whilst serpentinization of olivine can only take place below 400° C. Pressure was found to have little effect on reaction equilibria; the latter were almost entirely dependent on temperature. Bowen and Tuttle's main controversial statement, however, was that they did not detect a liquid phase below 1100° C. Therefore, theoretically, no magma of serpentine composition could exist below this rather elevated temperature. This would require a solid emplacement of such intrusive rocks as peridotites, dunites, and serpentinites. Bowen and Tuttle point out that due to the isolated SiO_4-type structures involved, minerals like olivine and serpentine might be expected to flow under high stress much more readily than the others (especially in high stress areas of alpine mountain systems). Once again, however, field observations are in direct contradiction with this hypothesis.

Roy and Roy (1954) synthesized serpentines and found that whilst temperature had little effect on which polymorph is produced, an increase in time favoured platy crystals. They also found that the presence of foreign ions (eg from Na Cl) increased the misfits in layers of brucite and silica, thereby favouring tube formation.

Gillery (1959) studied compositions giving the formula $(Si_{4-x}Al_x)(Mg_{6-x}Al_x)O_{10}(OH)_8$ with a range for x of 0 to 2.5, temperatures from 400 to 620° C, pressures of 15,000 to 56,000 psi, and times of a few minutes to 30 days. It was found that x = 0 compositions favoured the formation of fibrous serpentines (in contrast with the finding of Roy and Roy (op. cit.)). As x increased from 0, platy serpentines with one-layer ortho-cells were favoured, whilst a large value of x gave platy serpentine with 6-layer ortho-cells (6 (3) type). Cell parameters were also found to decrease with increasing x.

Hostetler et al. (1966), combining the previous experimental data of Bowen and Tuttle (1949), Yoder (1952) and Olsen (1963) with their field observations, suggested that the stability limits of olivine of Fo_{90} composition (rather than pure Fo olivines) be around 400° C at 15,000 psi water vapour pressure, such that:-

$$\text{olivine } (Fo_{90}) + H_2O + O_2 \xrightarrow{<400^\circ C} \text{clinochrysotile + brucite + magnetite} \quad (1)$$

and that the stability of clinochrysotile in the presence of magnetite be:-

$$\text{clinochrysotile + magnetite} \xrightarrow{<485^\circ C} \text{olivine } (Fo_{90}) + \text{talc} + H_2O + O_2 \quad (2)$$

They also noted that the widespread occurrence of brucite in Alpine serpentinites implied that temperature/pressure conditions during serpentinization are commonly those characterized by reaction (1) above, although a number of factors remain to be considered:

(a) the stability of lizardite rather than clinochrysotile,
(b) the influence of iron substitution in brucite and serpentine minerals,
(c) the presence of talc.

However, they concluded that a general serpentinization equation could be expressed by:-

$$\text{olivine} + H_2O + \text{silica} \xrightarrow{<500^\circ C} \text{"serpentine"}.$$

and that the presence of brucite demands large volume increases during serpentinization. To account for the latter, they assumed that serpentinization of Alpine ultramafics is accomplished by the addition of water during tectonic emplacement of the ultramafic bodies, and does not take place in situ after emplacement.

EXPERIMENTAL TECHNIQUES

X-ray Methods

At first, known polymorphs were studied using all available X-ray techniques, in an attempt to develop a rapid method for the subsequent processing of large numbers of specimens. Ideally, only single crystal photographs will identify all the polymorphs. However, this is a slow, nonroutine approach which is severely hampered by the lack of single crystals of macroscopic sizes. Efforts were therefore concentrated on powder methods, in the hope of increasing the usefulness of diffractograms from the limits previously imposed.

In this respect, Guinier and Debye-Scherrer film methods were evaluated against counter diffractometry. The latter has proved to be the most suitable instrument for detailed serpentine investigations. Numerous investigations have shown that it is impossible to obtain sharp powder diffraction patterns of the fibrous serpentines. This is due to preferential orientation, particle size, and internal crystal disorder. The implications of this complication are that:

(1) one has to be wary in making direct comparisons between diffractograms obtained by different methods, and with those of the literature.

(2) more unusual sample preparation techniques have to be used.

Three different counter diffractometer scans were made for each serpentine specimen. Initially, a rapid scan of the diffractogram was made (1/4° 2 θ /minute) on all specimens for preliminary identification. For the initial scan specimens were mounted on hollow holders in the form of a smear of fine powder on double-faced scotch tape. This mounting technique gave remarkably low background levels, permitting the use of counter full-scale deflections of very low values (1000 to 300 cps FSD) without obliterating small peaks with background noise.

Additional scans were then made (at 1/8° 2θ /minute, from 3° 2θ to 120° 2 θ, Ni-filtered Cu radiation) with specimens containing 5 per cent fluorite as an internal standard. Two methods of specimen mounting were attempted on specimen/internal standard mixtures, and although neither method proved totally satisfactory, the combination of the two methods provided an acceptable substitute for the quality generally expected from other, more ordered crystal species. Initially, finely powdered specimens were intimately mixed with epoxy resin, the latter was allowed to set, and the resulting briquettes ground to produce flat surfaces. This procedure helped in the elimination of preferred orientation of the crystallites, but caused a significant drop in the intensity of all reflections while increasing the background level substantially. This made it difficult and in some cases impossible to locate and measure accurately the weaker reflections. Other specimen/internal standard powders were smeared on double-faced scotch tape; this improved intensity of all reflections and allowed the weakest reflections to be located, but also produced strong preferred orientation effects which resulted in distorted relative intensities between different types of reflections.

Limits of Detection

The identification of the three most common serpentine polymorphs (chrysotile, antigorite, lizardite) depends on the careful observation of the shapes of the diffracted peaks at approximately 20°, 36° and 60° 2 θ (Cu radiation), as is shown in Figure 3. Examination of Figure 3 reveals that the peaks involved in the identification are of minor intensity and are relatively broad. Since admixtures of different polymorphs was expected to give major identification problems, synthetic mixtures were prepared containing varying amounts of the polymorphs, first as two-component mixtures, and later as three-component mixtures. Lizardite was found to be the most readily detectable, down to as little as 1 per cent by weight for any two or three component mixture. Antigorite could be detected down to 10 per cent by

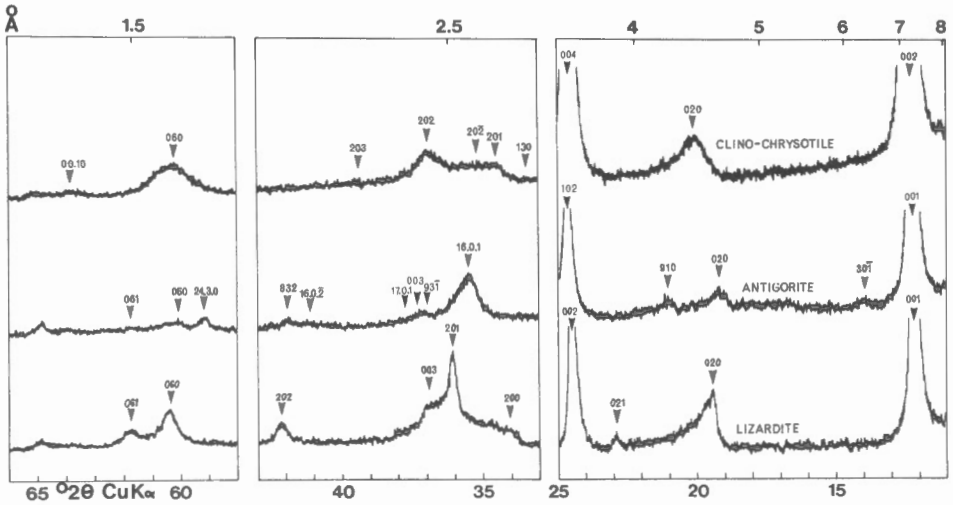

Figure 3. Standard diffractograms for pure clino-chrysotile, antigorite and lizardite, showing only the areas containing useful criteria for polymorph identification. Recorded at 1/4° 2 θ/minute, time constant = 3, 1 K c. p. s. full scale deflection, Cu K α radiation, Ni filtered.

weight in either lizardite or chrysotile (see Fig. 4 as an example), whereas chrysotile proved difficult to identify in concentrations of less than 20 per cent in the presence of either of the other polymorphs (the more fibrous nature of chrysotile could be identified more easily optically, however).

Similarly, the repeated occurrence of other minerals as impurities in the serpentine diffractograms forced a determination of the limits of detection of the associated impurities in the serpentine. Figure 5 represents a diffractogram of lizardite containing 1 per cent by weight of each of the 'impurities' chlorite, biotite, talc, tremolite and brucite. Similar diffractograms were prepared for concentrations of olivine, clinopyroxene, orthopyroxene, magnetite, calcite and dolomite. In every case a 1 per cent impurity is clearly visible, with detection limits extending considerably lower in many cases. Some interference may occur, however, as in the case where less than 1 per cent brucite is in the presence of more than 2 per cent chlorite, making the detection of the former more doubtful.

Hess and Otalora (1964) had produced similar quantitative mineral identification graphs, but in general their results could only be used in the rare instances when the 'impurities' occurred as major phases of 10 per cent by weight or more.

In the tabulations of the minerals detected in the diffractograms, which will be discussed later, trace amounts of impurities are generally taken to indicate 1 per cent or less by weight, whereas minor amounts indicate concentrations of between 1 and 5 per cent. On the other hand, minor amounts of accessory serpentine polymorphs within another serpentine phase indicate concentrations of 20 per cent or more for antigorite, and 40 per cent or more for chrysotile, both in lizardite hosts, whereas trace amounts (actually never reported) would have indicated concentrations around the detection limits discussed above.

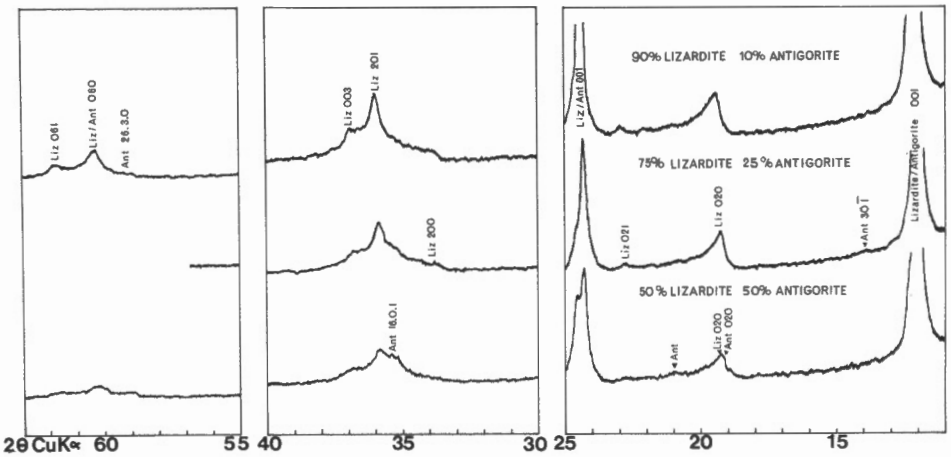

Figure 4. Diffractograms showing the effects of different concentrations of antigorite in a lizardite matrix recorded at 1/8° 2 θ /minute, time constant = 10, 1 K c. p. s. full scale deflection, Cu K α radiation, Ni filtered.

Specimen Selection

A representative series of specimens from the Muskox and Mount Albert intrusions were selected from material available at the Geological Survey of Canada, on which previous petrographic and chemical investigations had been carried out by Irvine and Smith (1967), Smith and Kapp (1963), MacGregor (1962), and Findlay and Smith (1965). Lack of direct involvement with the collection of specimens from these intrusions (Mount Albert especially is reflected in the scarcity of detailed petrographic descriptions for the rock types under investigation, although preliminary rock type identifications and descriptions are available in every case (tabulated here with the X-ray data). Specimens from the Jeffrey Mine were collected by the author in the summer of 1967, and are characterized both as to field appearance, rock type and exact location sampled; care was taken not to use asbestiform specimens for the main part of this study, but to restrict most of the investigations to the more massive serpentinized host rocks. Specimens from the Mid-Atlantic Ridge at 45° N were dredged by the author during the Bedford Institute 1968 cruise to the area on board C. S. S. Hudson (Cruise B. I. – 22 – 68 – Hudson).

Insufficient serpentinization of the parent intrusive rocks from Muskox, Mount Albert and Jeffrey Mine necessitated the separation of a light, nonmagnetic mineral fraction (S. G. <2. 84) from the whole rocks for the study of the serpentine polymorphs. The same procedure was adopted for the Mid-Atlantic Ridge specimens, but it was later realized that serpentinization of these rocks had progressed so far as to allow whole rock diffractograms to be made, and to make interesting comparisons between whole rock and serpentine concentrate diffractograms.

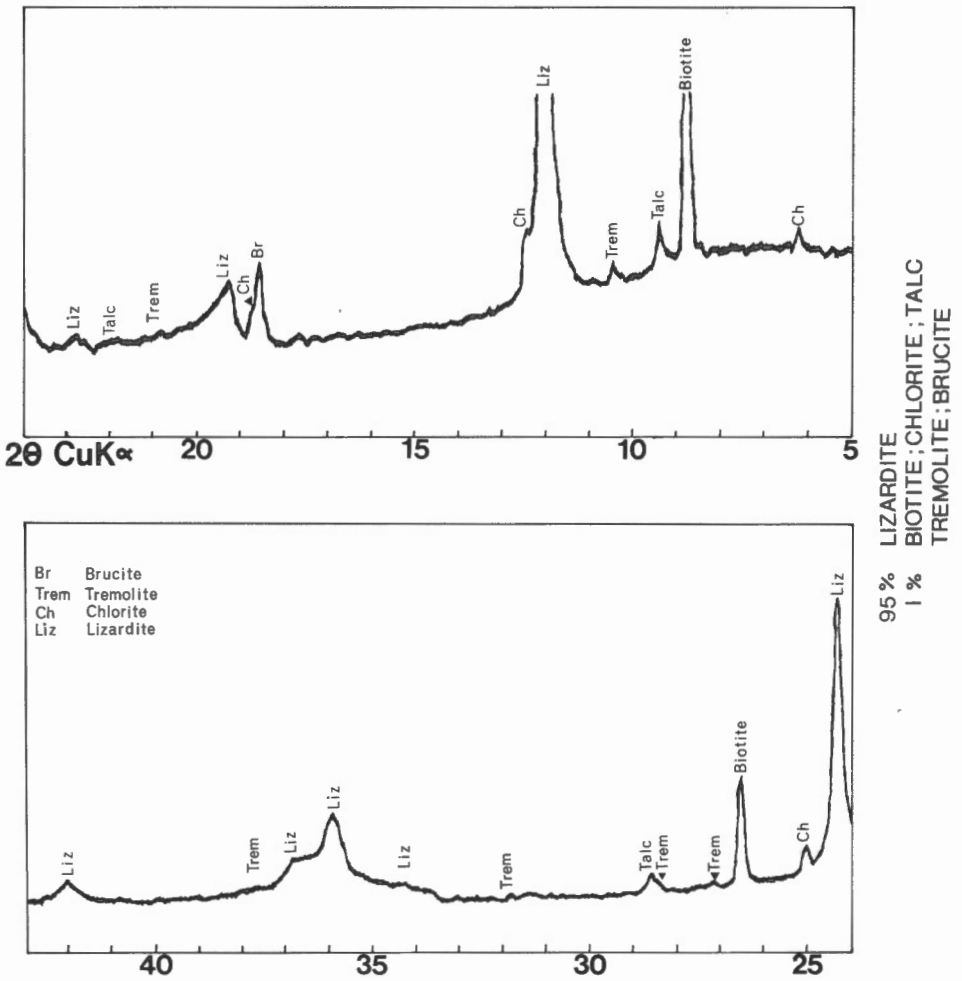

Figure 5. Diffractogram showing the possibilities of simultaneous identification of 1 per cent by weight of each of the impurities chlorite, biotite, tremolite, brucite and talc in a 95 per cent matrix of lizardite. Diffractogram recorded at 1/8° 2 θ /minute, time constant = 10, 1 K c. p. s. full scale deflection, Cu K α radiation, Ni filtered.

THE MUSKOX INTRUSION

The Muskox Intrusion is composed of a feeder, a marginal zone, and a central layered series (Irvine and Smith, 1967). The layered series is composed of rocks ranging from dunite to granophyre, and makes up the bulk of the intrusion. The serpentinite minerals from the lower half of the layered series (Fig. 6) were examined in this study. Twenty-one specimens were chosen from the core of the South Drill Hole between the 66- and 1,744-foot

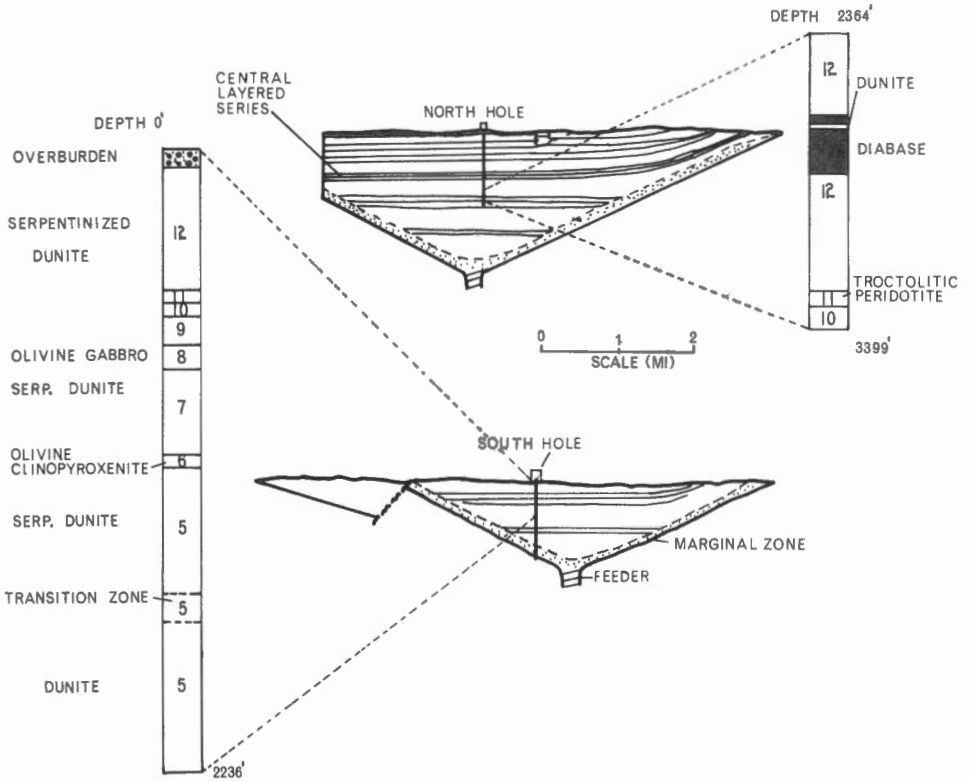

Figure 6. Generalized sketch map of the Muskox Intrusion showing positions of the boreholes, and specimen location.

depths (see Findlay and Smith, 1965, for the logs of the drillholes) and an additional 9 specimens were selected from the North Drill Hole core between the 2,563- and 3,267-foot depths. The latter specimens were all derived from a dunite layer (layer 12) and were chosen for comparison with specimens from the same dunite layer from the South Drill Hole.

The serpentine minerals studied were separated mainly from dunite (24 out of 30 specimens) but serpentines from olivine clinopyroxenites (3), troctolite peridotites (2) and an olivine gabbro (1 specimen) were also examined (see Table 1, Appendix). The olivine in these rocks ranges from 80 to 85 per cent Fo (Smith and Kapp, 1963) and the serpentine minerals formed from the olivine generally display a typical mesh texture with mesh rims of length-fast apparent fibres and mesh centres of relict olivine or isotropic or near isotropic serpentine. In many places the mesh texture is developed with preference for one set of mesh rims so that a banded growth, or curtain texture, of parallel sets of bipartite veins has developed (as described by Francis, 1956). Considerable quantities of magnetite are generally formed during the serpentinization process. Clinopyroxene is the only pyroxene present in the specimens studied. The clinopyroxene appears to alter to biotite or biotite and chlorite rather than serpentine (bastite). On examination

of thin sections it was possible to predict (after Wicks and Zussman, 1967) that lizardite was the serpentine mineral making up the mesh textures.

Muskox X-ray Results

Impurities in the Nonmagnetic Light Mineral Fraction

A persistent and surprising impurity in the, so-called, nonmagnetic light mineral fraction, was magnetite. Examination of the mineral grains in oil, under the microscope, revealed that most serpentine grains contained very finely divided specks of magnetite so that in most cases it was impossible to produce a nonmagnetic light mineral fraction. Exceptions to the magnetite contamination (see Table 1) were the serpentine formed in the troctolitic peridotites, and olivine clinopyroxenites, and some of the partially serpentinized dunite in Layer 5.

In most of the specimens, the olivine had been completely serpentinized, so that contamination by olivine did not occur very often. However, in a few layers, notably Layer 5, a dunite which was less serpentinized with depth, small amounts of olivine were detected in the concentrates.

The serpentine concentrates from the three olivine clinopyroxenite samples all contained large amounts of clinopyroxene (20 per cent or more) which obscured the serpentine diffraction pattern. Clinopyroxene was also present in lesser amounts in the troctolitic peridotite samples. The only other contaminants were biotite (or phlogopite) and chlorite, the alteration products of the clinopyroxene, although some of the biotite in the North Drill Hole samples may have been primary. The biotite and chlorite were mainly restricted to the dunite layers.

Serpentines and Related Minerals

Lizardite was the only serpentine mineral identified in the Muskox diffractograms. Previous limits of detection calibrations suggest that lack of positive identification of antigorite and chrysotile in a lizardite matrix indicates that antigorite and chrysotile may still occur in concentrations of less than 10 or 20 per cent by weight respectively, or may be completely absent. However, since there is no evidence for either chrysotile or antigorite in thin section, it is probable that neither is present in appreciable amounts. Similarly there is no X-ray or thin section evidence for the presence of 6-layer serpentine types.

Eight serpentine concentrates were of sufficient purity to permit accurate cell parameter measurements to be made. Indexed 'd' spacings and intensities are given in Table 2, Appendix. All but one of the specimens, S-0566.5, from a troctolitic peridotite, are from dunite layers. Cell parameters were computed from the indexed diffractograms (angular positions having been corrected with the CaF_2 internal standard) using a least squares refinement program. The refined cell parameters for lizardite are also given in Table 2, but the variations found can be summarized as follows:

	Maximum	Minimum	Average	Values from Rucklidge and Zussman (1965)	
a	5.333	5.315	5.322	5.31	Å
b	9.235	9.218	9.225	9.2	Å
c	7.317	7.309	7.313	7.31	Å

Considering the small number of diffraction peaks used in the cell parameter calculations (never more than 15), and the broadness of the peaks, especially at high 2θ angles, the limit of confidence on the parameters calculated is expected to be only $\pm$ 0.005 Å. However, observed and calculated 'd' spacings show considerably better agreement. Thus the values obtained indicate that small variations exist at least in the a and b parameters, suggesting that varying amounts of ionic substitution has occurred in the tetrahedral or octahedral sheets. Measured and calculated values involving the c parameter do not show such good agreement, making variations in c parameter more difficult to interpret.

The problem of preferred orientation of lizardite grains is well illustrated by the intensity measurements listed in Table 2. Intensity measurements were taken from diffractograms of (a) serpentine minerals on double-faced scotch tape smears, (b) serpentine minerals and internal standard on double-faced scotch tape smears, and (c) serpentine minerals and internal standard in epoxy resin mounts. Both the smear mounts gave identical results, so that only one such type of measurement is recorded in Table 2. The epoxy resin mounts gave the more random distribution of the mineral grains, resulting in stronger $h0\ell$ reflections relative to the 00ℓ reflections, but with an overall reduction in intensity that made accurate measurement of the weaker reflections very difficult. One curious feature of the two different mounting techniques is the consistent shift of the $hk\ell$ 002/004/006 intensity ratio from 100/42/4 for the double-faced scotch tape mounts to 100/52/5 for the epoxy resin mounts.

Brucite is not a common mineral in the Muskox specimens. It occurs in very minor amounts (1 per cent or less) in only 5 of the 24 dunites. It is present in trace amounts in three other dunites, and is possibly present in 5 others. It does not occur in the olivine clinopyroxenites, troctolitic peridotites or olivine gabbro.

In 4 out of 5 dunite specimens from Layer 12 in the South Drill Hole strong reflections are present at 7.8, 3.90 and 2.62 Å superimposed on the lizardite diffractogram. Hess and Otalora (1964) found similar reflections in their X-ray work on the specimens from the AMSOC drillhole in Puerto Rico. They did not give the mineral a name but believed it to be similar to a nickeliferous magnesium hydroxide from Pennsylvania, later described by Lapham (1965) to be a nickeliferous polytype of brucite of essentially the same structure as pyroaurite (approximate composition $Mg_6Fe_2(OH)_{16}(CO_3).4H_2O$. The diffraction pattern of the mineral associated with the Muskox lizardite is similar to that of pyroaurite, and is tentatively identified as such. Pyroaurite was not detected in specimens from Layer 12 in the North Drill Hole.

Similar additional sets of weak reflections at 8.1 and 4.06 Å occurred in diffractograms from most of the dunite specimens, in one of the troctolitic peridotite and possibly in one of the olivine clinopyroxenite specimens. These were attributed to minor or trace concentrations of brugnatellite ($Mg_6 Fe (OH)_{13} CO_3.4H_2O$).

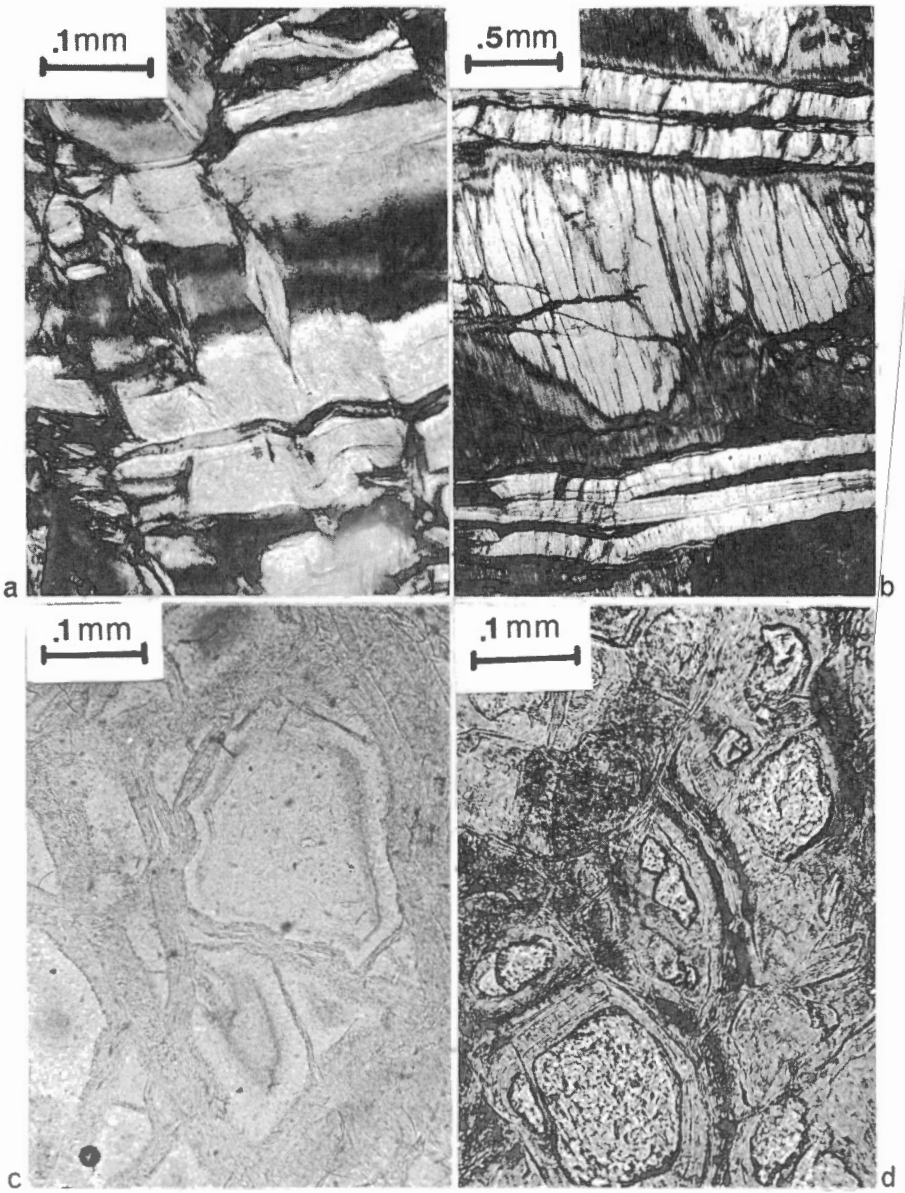

Figure 7. Mount Albert photomicrographs

(a) Olivine and orthopyroxene serpentinized to give curtain and mesh textures, possibly altered by shearing (111360).

(b) Large orthopyroxene replaced by chrysotile exhibiting curtain texture subparallel to the orthopyroxene cleavage, later cut by chrysotile veinlet (111365).

(c) Sheaf-like curtain texture of lizardite pseudomorphic after olivine (111384).

(d) Olivine altered to curtain textured lizardite (111358).

THE MOUNT ALBERT INTRUSION

The Mount Albert Intrusion is an Alpine ultramafic intrusion composed mainly of peridotite and dunite. It is somewhat unusual in that, unlike most Alpine-type ultramafic intrusions, it has a high-temperature metamorphic aureole. The composition of the olivines varies from 90-92% Fo, and the enstatite from 91-97% En (MacGregor, 1962). The serpentine minerals derived from the olivine display characteristic mesh textures with mesh rims of length-fast apparent fibres and mesh centres of nearly isotropic serpentine or relict olivine (Fig. 7). The serpentine derived from the enstatite forms bastites, serpentine pseudomorphs composed of length-slow serpentine fibres lying parallel to the original enstatite cleavage. Secondary minerals include chlorite, generally associated with the chrome-spinels and their alteration products, and tremolite and talc.

Most of the rocks selected for this study were peridotites although 4 or 5 peridotite/dunite transitional rocks were included. In choosing samples an effort was made to select as representative a sample distribution as possible, but this was limited by the fact that, in almost all cases, the rocks chosen had to be over 50 per cent serpentinized in order to get a reasonably pure serpentine concentrate. Rocks that were less than 50 per cent serpentinized did not yield pure enough concentrates and even those between 50 and 90 per cent serpentinized generally contained minor but appreciable impurities. Figure 8 shows the general outlines of the intrusion with superimposed zones of equal degrees of serpentinization and specimen locations.

Thin section studies suggested that the mesh textures observed were composed essentially of lizardite, and the bastite to be composed essentially of chrysotile. Since most of the rock specimens contained less than 10 per cent enstatite, and in many cases this was not completely serpentinized, it was expected that chrysotile would occur in insufficient concentrations to make it detectable by X-ray diffractometry.

Mount Albert X-ray Results

Impurities in the Nonmagnetic Light Mineral Fraction

The ubiquitous presence of at least small amounts of olivine and/or enstatite (see Table 3, Appendix) in the concentrates masked a number of the characteristic peaks of the serpentine minerals. Hand picking of the mineral grains failed to eliminate the problem, suggesting that the olivine and enstatite grains occur as composite grains with cores of the relict minerals surrounded by serpentine. In contrast to the Muskox contaminations, magnetite did not occur in an intimate association with the serpentinite, so that the concentrates were always found to be completely nonmagnetic.

Other minerals which were identified on the diffractograms were accessory chlorite, talc and amphibole. Again in contrast to the Muskox data, biotite and clinopyroxene were completely absent.

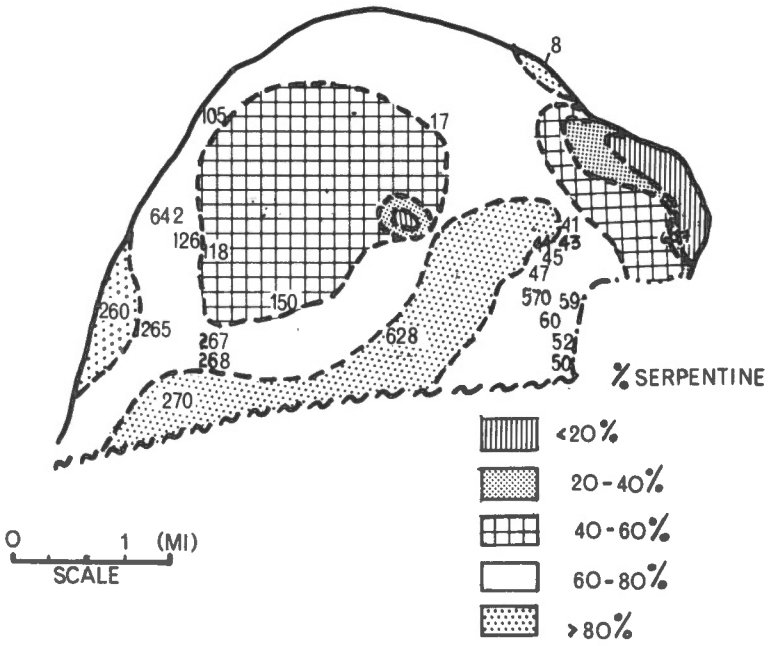

Figure 8. Generalized sketch map of the Mount Albert Intrusion, showing zones of equal degrees of serpentinization, and location of specimens.

Serpentines and Related Minerals

Lizardite was the only serpentine mineral identified in the Mount Albert concentrate diffractograms. Chrysotile, which was thought to make up the bastites, was not detected, presumably because it either occurred in concentrations of 20 per cent or less, or did not occur at all. No antigorite or 6-layer serpentines were detected.

Seven concentrates were sufficiently pure to permit accurate cell parameter measurements (see Table 4, Appendix, for details). Least squares refinements gave the following parameter variations:

	Mount Albert			Muskox	Values from Rucklidge
	Maximum	Minimum	Average	Average	and Zussman (1965)
a	5.343	5.317	5.328	5.322	5.31 Å
b	9.248	9.218	9.230	9.225	9.2 Å
c	7.312	7.302	7.307	7.313	7.31 Å

Slight differences in parameters exist between the Mount Albert and Muskox lizardites; the former tend to exhibit larger a and b and smaller c parameters, but variations are slight. The Mount Albert lizardites may therefore exhibit greater degrees of ionic substitutions of Si by larger ions to expand the tetrahedral sheets.

Brucite is a persistent accessory mineral in most samples. It is present in significant amounts (more than 1 per cent) in 15 of 30 samples, is detectable in 7 others, cannot be observed due to the interference of chlorite in 5 samples, and is only definitely not present in 3 out of the total of 30 samples. Pure magnesium brucite has an 001 d-spacing of 4.77 Å (ASTM 7-239). The 001 reflections from the Mount Albert samples range from 4.76 to 4.70 Å and in some cases (SDM57-44, Table 4) two peaks are resolved, one at 4.76 and a second at 4.70 Å. This may suggest that iron is substituting for magnesium in some of these brucites. Iron bearing brucites in Alpine serpentinites have been reported by Hostetler, et al. (1966).

Brugnatellite is also a common accessory mineral, although it generally does not give as intense a diffraction pattern as brucite. It is identified by two reflections, at 8.1 and 4.05 Å. It is present in significant amounts in 5 samples in trace amounts in 15 and probably in 4 others. It is only absent in 6 of the 30 samples. In two samples, SDM57-43A and SDM57-270, very weak reflections at 7.8 and 3.90 Å indicate very minor amounts of pyroaurite.

JEFFREY MINE, ASBESTOS, QUEBEC

The Jeffrey Mine is an open pit operation excavated into the serpentinized peridotite section of a differentiated ultrabasic intrusive sill. The sill was intruded concordantly into stratified rocks of early Paleozoic age in late Ordovician times. The sill, which is 4,800 feet thick, consists of peridotite, dunite, pyroxenite and gabbro. All these rock types have been serpentinized to varying degrees. The serpentinized peridotite underlies most of the open pit mine, where it is considered to be the ore bearing rock type and is divided into five ore zones, numbered from 1 in the north-northwest in intrusive contact with the footwall slates, to 5 in the south-southeast at the hanging wall with the overlying serpentinized dunite. The dunite is considered to be barren of ore grade serpentine. The dunite is interfingered by concordant pyroxenite lenses, and eventually grades into gabbro at the extreme south-southeast of the sill, where it is in intrusive contact with Cambrian or Ordovician volcanics. A simplified topographic and geological map of the mine is presented in Figure 9, where sample locations are also given.

The peridotites show colour variations from light green-grey to a dark, almost black, green, generally weathering to a buff colour. Thin sections reveal that the olivines are almost entirely altered to serpentine, producing the typical mesh textures also observed in the Muskox and Mount Albert rocks. Bastite and pyroxene together average about 10 per cent of the rock, and locally reach a maximum of 35 per cent. The bastite is easily visible in hand specimen, and the local variations in serpentinization give the rocks a mottled appearance. The peridotites are often cut by veins of cross and slip fibres, composed mainly of chrysotile. The serpentine ore is derived primarily from these fibre zones and from concentrations of mass fibre, the latter often accompanied by brucite occurring as small, disseminated flakes.

Specimens were collected from zones 1 to 5 in the peridotite on both the east and west walls of the pit, and from the waste zone in the dunite on the south wall. A number of drill cores were also collected from hole

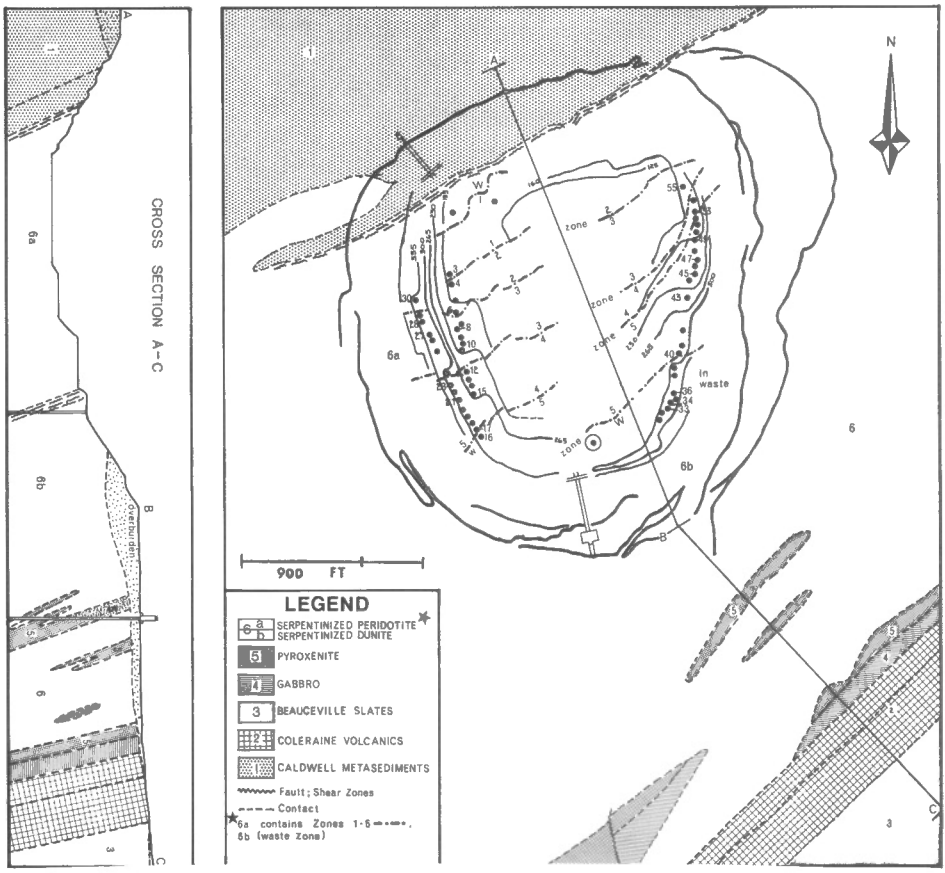

Figure 9. Generalized sketch map of the Jeffrey Mine, Johns-Manville Co. Ltd., Asbestos, Que., showing subdivision of serpentinized peridotite into five ore zones, and location of specimens.

No. 621 (see Fig. 9) which passes through the dunite waste zone into the peridotite zone 5 beneath. A total of 25 specimens were selected from the above, 21 of which came from the peridotite, and 4 from the waste zone 'dunite'. Five specimens of peridotite containing chrysotile-rich cross fibres were also included for comparison.

Jeffrey Mine X-ray Results

Impurities in the Nonmagnetic Light Mineral Fractions

The concentrates were relatively free from impurities (Table 5, Appendix), suggesting that serpentinization of individual minerals, where it had commenced, had gone to completion without leaving unaltered remnant cores of the original minerals. Only one specimen contained minor amounts of olivine, whereas three others had trace amounts of olivine (less than 1 per cent). Similarly one specimen contained minor amounts of enstatite, whilst

three other bastite-rich specimens showed traces of enstatite. A trace of magnetite was detected in only one concentrate (the only one showing magnetite in hand specimen also), whilst biotite, clinopyroxene, and tremolite were nonexistent.

Serpentines and Related Minerals

Chrysotile and antigorite were detected for the first time in this study, but lizardite retained its position as the most common serpentine polymorph. Out of 12 chrysotile detections on diffractograms (indicating concentrations of 20 per cent or more) 5 were from peridotites containing visible cross-fibre veinlets, 3 from peridotites with visible concentrations of mass-fibre, and three from peridotites with unusually high concentrations of bastites. Only one peridotite without obvious visible chrysotile concentrations (no major bastite concentrations, cross- or mass-fibres) contained minor chrysotile. In addition, two peridotites, one with mass-fibres, the other with the magnetite-rich slip-fibres, gave minor concentrations of antigorite. Lizardite is therefore the predominant polymorph in the Jeffrey Mine also, except for the instances where obvious secondary asbestos mineralization has produced chrysotile, and where minor slippages have formed antigorite.

Ten specimens were selected for cell parameter measurements (see Table 6, Appendix). Least squares refinements gave the following parameter variations:

	Jeffrey Mine					Values from
	Maximum	Minimum	Average	Mount Albert Average	Muskox Average	Rucklidge and Zussman (1965)
a	5.365	5.311	5.333	5.328	5.322	5.31 Å
b	9.246	9.191	9.226	9.230	9.225	9.2 Å
c	7.356	7.277	7.318	7.307	7.313	7.31 Å

The Jeffrey Mine lizardite parameters are generally larger than for both the Muskox and Mount Albert specimens although a couple of smaller values tend to lower the average values considerably.

In an additional, but complementary study, a search was made for the less common polymorph by hand picking serpentine minerals from the walls of the Jeffrey Mine where it was possible to collect larger crystals showing morphological characteristics more clearly. Most of the fibrous serpentines collected proved to be pure clinochrysotile, with only a few specimens showing admixtures of clino-chrysotile with minor amounts of ortho-chrysotile. Of the platy serpentines, the majority were antigorite, with only a small percentage of ortho-serpentine of the 6(2) variety. It must be stressed, however, that these less common polymorphs were found only during this more selective, independent search, and that they occur under such conditions and in such minor quantities as to suggest that they are not essential constituents of the more massive serpentinized peridotites; in any case they would be undetectable by the routine X-ray examination of concentrates.

Talc was only found in one specimen, where it had been previously identified both in hand specimen and in thin section. The same specimen also contained chlorite; the latter also occurred in minor or trace amounts

(in any case, less than 1 per cent) in three other peridotites. Brucite concentrations were very variable; it occurred in at least 12 specimens (both in the more massive peridotites, and in those with veinlets); on 6 of these occasions it occurred in concentrations greater than 5 per cent, in 5 others between 1 and 5 per cent, and in the 12th specimen in trace concentrations (less than 1 per cent). Brucite was absent in the remaining 13 specimens.

Twelve specimens showed minor to trace concentrations of brugnatellite, whereas pyroaurite possibly occurred as traces in only two specimens, if at all. Both pyroaurite and brugnatellite, and the other associated minerals showed no correlation between occurrence and peridotite zonation, although the Waste Zone dunites were generally of remarkably pure lizardite content.

THE MID-ATLANTIC RIDGE

The deep ocean basins, which cover two-thirds of the earth's surface, are dominated by three large scale structural elements: (a) the mid-ocean ridges which have approximate median positions within them, and which are associated with active seismicity, (b) the major fracture zones, which traverse the mid-ocean ridges, often offsetting their crests, and (c) the trench systems of the island arcs.

The axes of mid-oceanic ridges are thought to be the loci at which new crustal material is generated by the upswelling and outpouring of large quantities of basaltic lava. The origin of the basalt is not yet clear, but may be either the molten equivalent of primitive material in the earth's mantle, or may only be a differentiate (by partial melting?) of primitive mantle material (such as peridotites or other ultrabasic rocks). Seismic data suggests that the basalts which make up Layer 2 of the ocean floor crust are underlain by serpentinized peridotites in Layer 3. Dredge data from fracture zones, where it is reasonable to suppose that the more deep-seated layers are exposed, supports the seismic hypotheses to a certain extent. However, the dredge data suggest that the seismic picture is somewhat oversimplified, since, although serpentinized peridotites are the most abundant rock types collected, gabbros and metamorphosed basalts are also common. The peridotites are commonly thoroughly serpentinized, to a far greater extent than the peridotites found in continental ultrabasic intrusives (e. g., Muskox and Mount Albert); in the past the high degree of serpentinization has been attributed to the fact that the localities sampled are, by necessity, along the fracture zones themselves, where additional serpentinization may be expected to take place.

The method of emplacement of the peridotite layers of the ocean floor, and their subsequent serpentinization, is unknown. A thorough study of the serpentinites from a mid-oceanic ridge, and comparison of data with better understood continental occurrences, may thus be of great importance towards the elucidation of mid-oceanic tectonics.

The Mid-Atlantic Ridge at 45° N was sampled by the author at over 40 positions (Fig. 10). Out of these, eight localities yielded major amounts of highly serpentinized basic and ultrabasic rocks. Three of these localities were on elongated, block-faulted seamounts, where similar conditions to the serpentinized peridotite occurrences on fracture zones may be presumed to

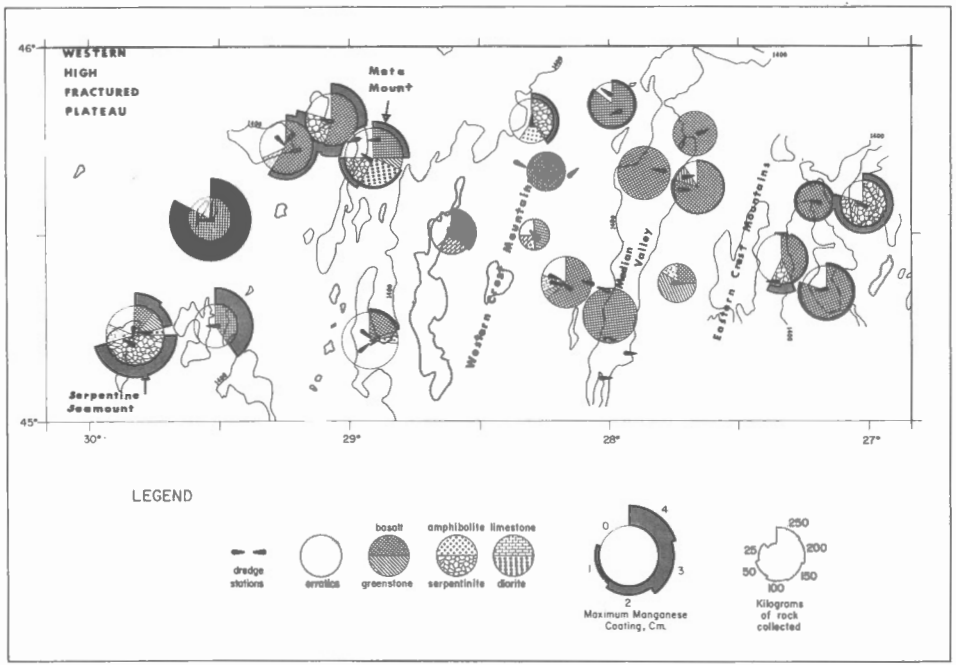

Figure 10. Bathymetry of the Mid-Atlantic Ridge at 45° N, showing only the 1400 formation contour, delineating the major topographic features. Superimposed are the dredge station locations, and specimen yields.

exist (i. e., the fault scarps have exposed more deep-seated layers, such as the seismic Layer 3); the remaining five localities, however, are on seamounts of more conical outlines, which suggest shield-type volcanoes or diapiric intrusives rather than block-faulted features. The bathymetry of the Mid-Atlantic Ridge at 45° N is represented in a simplified, schematic way in Figure 10, which also shows the dredge locations and major structural subdivisions of the area. It is interesting to note that the Median Rift Valley and its associated fault scarps, which have some of the largest throws in the area, never yielded any serpentinized rocks, but in one instance, at the very foot of a major fault scarp, yielded gabbros; in addition, pillow lava from the area contains abundant plagioclase and olivine xenocrysts, which are evidence of gravity differentiation of crystallizing magmas somewhere beneath the pillow lava (Aumento, 1968

The high degree of serpentinization obscures most of the original mineralogy of the rocks dredged from the area. However, relict structures are well preserved which, together with the few remnant unaltered minerals, permits the identification of the original rock types. Most of the parent rocks were identified as harzburgite peridotites, some of the specimens retaining evidence of layering, especially in cases exhibiting chromite layering. Other rocks include amphibolitic peridotites (possibly related to similar rock types described by Tilley, 1947, from St. Paul's Rocks, Atlantic Ocean), troctolitic gabbros, and dunites. All the different rock types could be found on one of the block-faulted seamounts, strongly suggesting that the fault plane has exposed something akin to a layered ultrabasic complex.

Chemical and spectrographic analyses for the Mid-Atlantic Ridge serpentinites are given in Tables 7 and 8 (Appendix) to assist in the characterization of these previously unstudied specimens. The analyses show little variation (except for those exhibiting high CaO values due to organic contamination), and are quite similar to analyses of serpentinites from Mount Albert (MacGregor, 1962) and the Mayaguez Drill Hole in Puerto Rico (Hess and Otalora, 1964). However, the Mid-Atlantic Ridge serpentinites exhibit consistently higher Al_2O_3/CaO ratios (due primarily to extremely low CaO contents).

Concentrates from 13 representative specimens were prepared in the same way as for the other serpentinites studied. However, it later became evident that serpentinization had progressed to such an extent that whole rock specimens could be ground up and X-rayed with equal success; whole rock powders from specimens which had previously been X-rayed as concentrates were re-examined and the two sets of results compared, and in addition, 6 additional whole rock specimens were run.

Mid-Atlantic Ridge X-ray Results

Impurities in the Whole Rocks and in the Nonmagnetic Light Mineral Fractions

The advanced degree of serpentinization is immediately evident from Table 9 (Appendix). The concentrates showed only three occurrences of trace amounts of olivine and enstatite, and two of tremolite. Biotite, clinopyroxene and magnetite were completely absent. The whole rock diffractograms reproduced the data from the concentrates very closely, except for their indication

of the presence of magnetite and carbonate (both calcite and dolomite, contaminants of possible organic origin), and the higher concentrations of tremolite from the amphibolitic peridotite specimen. Therefore, the degree of serpentinization has exceeded 95 per cent in most cases.

Serpentines and Related Minerals

Lizardite again proved to be the dominant serpentine polymorph. Only one occurrence of antigorite was found, in a specimen showing strong brecciation (similar conditions to the antigorite occurrences in the Jeffrey Mine). Similarly, chrysotile occurred in three harzburgites, two of which were strongly brecciated.

Brugnatellite occurred in trace concentrations in only three specimens, whereas pyroaurite was completely absent. Brucite was also rare, with four occurrences in trace concentrations. Talc was primarily restricted to the sheared specimens, where concentrations of 1 per cent or more could be found, but also occurred in trace concentrations in two other harzburgites.

Ten lizardites gave sufficiently good diffractograms for precise cell parameter measurements (Table 10, Appendix). The range of values obtained is as follows:

	Mid-Atlantic Ridge			Muskox	Mount Albert	Jeffrey Mine	Values from Rucklidge and
	Maximum	Minimum	Average	Average	Average	Average	Zussman (1965)
a	5.334	5.306	5.317	5.322	5.328	5.333	5.31 Å
b	9.220	9.204	9.210	9.225	9.230	9.226	9.2 Å
c	7.286	7.313	7.301	7.313	7.307	7.318	7.31 Å

The Mid-Atlantic lizardites give consistently lower cell parameters than do the Lizardites of the continental intrusions. The a and b parameters especially seem to form a series of increasing size, commencing with the smaller Mid-Atlantic Ridge lizardites, through the intermediate Muskox lizardites, to the larger Mount Albert and Jeffrey Mine lizardites.

ANALYSIS OF X-RAY DATA

Minerals Unrelated to Serpentinization Processes

Before analysis of the mineral data collected is made, a number of the accessory minerals are first discussed and then discarded from further consideration due to their more obvious secondary nature, not directly related to the processes of serpentinization. Under this classification, the carbonates detected in the Mid-Atlantic Ridge specimens can be eliminated, for there is evidence that they are of organic origin, deposited in cracks by organic action on the sea floor. Oxygen isotope ratios of these carbonates have delta values indicative of formation in cold, deep-sea conditions (K. Muehlenbachs, University of Chicago, pers. comm.).

Similarly, pyroaurite, which is found only in the upper 400 feet of the South Drill Hole in the Muskox Intrusion (and in very minor amounts in a few Mount Albert and Jeffrey Mine specimens) is thought to be produced by

weathering or action of groundwater on serpentinites, and thus is not related to the processes of serpentinization (Hostetler, et al., 1966).

In the evaluation of the primary serpentinization processes to follow, the occurrence of chrysotile and antigorite in the Mid-Atlantic Ridge and Jeffrey Mine specimens is not considered, since in most cases where these two polymorphs were detected, there was evidence of secondary movements affecting the rocks; these cross-fibre, slip-fibre and mass-fibre veins and associated brecciations are known to be directly related to the formation of chrysotile and antigorite subsequent to the main serpentinization processes.

Minerals Related to Serpentinization Processes

Table 11 (Appendix) attempts to condense all the X-ray data collected by reporting only approximate values of the mineral concentrations detected in the concentrates averaged for each intrusion.

It has already been shown that serpentinization of intrusions of different compositions, ages and tectonic settings has consistently resulted in the formation of lizardite as the predominant serpentine polymorph. However, once initiated, serpentinization of individual mineral grains (as opposed to the rock as a whole) has been most effective on the Jeffrey Mine peridotites, resulting in the almost complete serpentinization of the primary olivines and pyroxenes. At the other extreme, in the Mount Albert peridotites there remain numerous relic pyroxenes and olivines in the cores of lizardite.

Temperature Considerations

Cell parameter variations, although slight, are the only differences found between the lizardites from different intrusions. There is a definite tendency for the Mid-Atlantic Ridge lizardites to exhibit the smaller parameters, and for the larger parameters to occur in the Mount Albert and Jeffrey Mine lizardites. It is unfortunate that in previous work on synthesizing serpentines no stress was given to the accurate measurement of cell parameters or to factors controlling their minor variations (with the possible exception of Gillery, 1959). Direct comparisons and deductions are therefore impossible, but the general trends found with other mineral groups may be utilized here. In general, in the synthesis of a new phase from an impure matrix which only approximates the composition desired, the higher the temperature of crystallization of the new phase (other factors being equal), the more ordered is the structure to be expected. The higher temperatures will reduce the amounts of ionic substitution, especially 'stuffing' of crystal structures by larger cations.

In lizardite, the most common substitutions to occur are those of Si replacement by the larger Al, and Mg by the smaller Al or larger Fe^2. Assuming that temperature effects on these substitutions follow the general guidelines just described, increasing temperatures should reduce the substitution of Al into the Si positions and Fe^2 in the Mg positions, and simultaneously aid the substitution of Al into the larger Mg positions. The combined effect of these trends would be to produce considerable reductions in the 'a' and 'b' parameters with temperature. Their effects on the 'c' parameter would be more difficult to evaluate.

The smaller parameters found in the Mid-Atlantic Ridge lizardites may thus reflect higher temperatures of serpentinization, followed by slightly cooler conditions in Muskox, with the coldest conditions occurring at Jeffrey Mine and Mount Albert.

Similar temperature deductions may be made from a study of the accessory mineral assemblages (Table 11) in the light of previous experimental evidence by Bowen and Tuttle (1949) and Hostetler et al. (1966) discussed earlier in this work. Recapitulating, the presence of brucite in serpentinized ultramafics indicates a progressive lowering in the temperature of serpentinization by as much as 100° C from the maximum value of 500° C given for the reaction:

$$\text{olivine} + H_2O + \text{silica} \rightarrow 500° \rightarrow \text{'serpentine'}$$

The abundance of brucite may thus be taken as an indication of the 'coolness' of the main serpentinization process. The high brucite content of the Mount Albert serpentinites (typical of Alpine peridotites) suggests temperatures of serpentinization close to or below the possible maximum of 400° C; by similar reasoning the Muskox serpentinization occurred at relatively higher temperatures, possibly between 400° C and 485° C, and the Mid-Atlantic Ridge serpentinization, with its extremely low brucite content, occurred closer to the maximum temperature of 485° C. Two alternative explanations are possible for the temperature differences: (a) On the assumption that the four ultramafic bodies were intruded under hot, fluid conditions, then serpentinization may have been due to autometasomatic processes during the cooling cycles of the intrusions. The differences in temperatures would then be a reflection of both the sizes and tectonic settings of the different bodies. The smaller intrusions of the Mount Albert and Jeffrey Mine bodies would tend to cool more quickly, whereas the larger size of the Muskox Intrusion suggests a slower rate of cooling. The sizes of the Mid-Atlantic Ridge bodies are unknown, but if one assumes that Layer 3 of the ocean floor consists primarily of serpentinized peridotite and gabbro then the dimensions involved are considerably larger than for any of the Alpine-type or even the stratiform intrusions. Extremely slow rates of cooling would be expected from such bodies. (b) The previous deductions presume a hot intrusive stage for each of the bodies discussed. Serpentinization in situ would then revive the well discussed problems of whether volume changes or transfer of material have taken place; there is little evidence for the latter (Turner and Verhoogen, 1960; Coleman, 1965), but there are many possible occurrences of the former (Hostetler et al., 1966; Busé and Watson, 1960; Raleigh, 1963), including the possibility that the Crest Mountains of the Mid-Atlantic Ridge are elevated relative to the surrounding topography by volume expansion due to the serpentinization of the peridotite layers. Volume expansion would require that serpentinization take place during the diapiric intrusion of the peridotite masses of the Alpine type (e. g., Hostetler, et al., 1966); but in the layered intrusives, serpentinization at this stage would be impossible because magmatic differentiation by crystal settling had to take place after intrusion and before serpentinization. It is thus feasible that the temperatures of serpentinization are more a reflection of the conditions of intrusion of the different bodies; the smaller alpine bodies were intruded in partly crystallized and hence cooler conditions, with serpentinization taking place contemporaneously with or very soon after intrusion, whereas the stratiform Muskox body was intruded in a totally fluid and hot condition, and serpentinization

occurred on cooling. The Mid-Atlantic Ridge bodies may approximate the Muskox conditions, with an additional higher temperature factor resulting from the igneous activity on the oceanic ridge crest with its associated anomalously high heat flow values.

Compositional Considerations

Magnetite is generally abundant in the Muskox and Mid-Atlantic Ridge specimens where it forms an integral part of the serpentine minerals, making separation impossible. In the Mount Albert and Jeffrey Mine specimens it is far less abundant, and may be completely eliminated from serpentine mineral concentrates. It is felt that the difference in fayalite content between the Muskox and Mid-Atlantic Ridge olivines and those in the Jeffrey and Mount Albert serpentinites is insufficient to account for such marked variations in magnetite distribution. It is more probable that since serpentinization in the Mid-Atlantic Ridge and Muskox intrusions occurred above the stability field of brucite, the excess iron expelled from the serpentine matrix was not used up, and hence crystallized as distinct grains of magnetite. On the other hand, in the Mount Albert and Jeffrey intrusions, the simultaneous formation of lizardite and brucite led to the assimilation of excess iron by the crystallizing brucite to give iron-rich brucites, leaving little free magnetite. Indeed, the 'd' spacings of the brucites from Mount Albert (Table 4) and Jeffrey Mine are smaller than those for a pure magnesium brucite, indicating the possibilities of appreciable iron content.

The presence of brugnatellite in all but the Mid-Atlantic Ridge intrusions (occurs in very minor concentrations in the latter) is of considerable importance. Brugnatellite, composed of water molecules and carbonate groups lying between iron-bearing brucite layers, is indicative of very small concentrations of CO_2 in the water involved in the serpentinization. The partial pressure of CO_2 must in any case have remained below 0.5 mol % since above such a value brucite becomes unstable and the serpentine-brucite assemblage is replaced by serpentine-magnesite. Further increases in partial pressures of CO_2 cause serpentine to break down to talc and magnesite. The Mid-Atlantic Ridge serpentinizing waters are thus thought to have been remarkably free of CO_2.

CONCLUSIONS

The serpentine polymorph lizardite has been shown to be the predominant mineral formed in the serpentinization process of both ultramafic and mafic rocks of Alpine, stratiform and mid-oceanic ridge intrusive settings. The formation of lizardite is therefore independent of such factors as tectonic settings, chemical composition of the parent rock types, and major chronological differences. However the different cell parameters measured for lizardites from different intrusive bodies may be indicative of different degrees of ionic substitution within the lizardite lattice, and hence of different temperatures of serpentinization. The hottest temperatures (near 485° C) may thus have occurred on the Mid-Atlantic Ridge, intermediate to hot temperatures in the stratiform Muskox Intrusion, and the coolest temperatures (400° C or less) in the Alpine type intrusions of Mount Albert and Jeffrey Mine.

The different serpentinite bodies are characterized by the following accessory mineral suites:

(a) Muskox: brugnatellite, biotite and magnetite, with trace amounts of brucite, chlorite, olivine and clinopyroxene.
(b) Mount Albert: brucite, olivine, and enstatite, with traces of brugnatellite, chlorite, talc and tremolite.
(c) Jeffrey Mine: brucite, with traces of brugnatellite, chlorite, talc, olivine and enstatite.
(d) Mid-Atlantic Ridge: chlorite and magnetite, with traces of brugnatellite, brucite, talc, biotite, olivine, clinopyroxene, enstatite and tremolite.

Supporting evidence for the above-mentioned varying degrees of temperature of serpentinization is provided by the substantial concentrations of brucite found in the Mount Albert and Jeffrey Mine serpentinites (indicative of low serpentinization temperatures) and its virtual absence in Muskox and Mid-Atlantic Ridge serpentinites (suggesting temperatures approaching the maximum for the serpentinization reaction).

Differences in temperatures of serpentinization reflect both the variations in sizes, and hence the cooling rates, of the intrusions, and the times at which serpentinization took place relative to emplacement. In the Alpine type intrusives serpentinization probably occurred contemporaneously with the emplacement of a cool, semicrystalline ultrabasic mass, whereas in the stratiform intrusives serpentinization probably occurred on cooling after emplacement and after termination of the processes of differentiation by crystal settling. In the mid-oceanic ridges, serpentinization is also thought to have taken place after emplacement, but there is still insufficient evidence to determine whether differentiation of the magmas by crystal settling took place primarily before or after emplacement. However, the evidence found for layering suggests that much of the differentiation took place in situ after emplacement. Consideration of the tectonic models offered by seismic and heat flow experiments over the axis of the Mid-Atlantic Ridge (Keen and Barrett, 1969), and of the dredge yields obtained by the author, implies that magma differentiation may take place beneath the floor of the Median Rift Valley, and that, on solidifying, the rocks so produced are upthrusted as large blocks from the Median Valley floor to new positions forming the Crest Mountains. Only repeated upthrusting will expose the deeper, differentiated ultrabasic layers, thereby explaining why ultrabasics are not found on the fault scarps of the Median Rift Valley (where throws of up to 1 km expose gabbros only) but are common on faulted blocks farther removed from the axis. In those more remote areas repeated upthrusting may be expected to have taken place, exposing both the gabbros and the deeper peridotites as well as metamorphosed basalts.

The similarities between the Mid-Atlantic Ridge serpentinites and those from Muskox, and the evidence for differentiation by crystal settling in the former suggest that considerable affinities may exist between the two tectonic settings. The Mid-Atlantic Ridge serpentinites may thus be envisaged as being the product of the serpentinization, on cooling, of large stratiform differentiated bodies of ultrabasic to basic composition.

The presence of brugnatellite in the Muskox, Mount Albert and Jeffrey Mine serpentinites indicates that small amounts of CO_2 were present in the serpentinizing waters of these intrusions, whereas none was present in the Mid-Atlantic Ridge waters.

ACKNOWLEDGMENTS

The author is indebted to F. J. Wicks, research student in the Department of Mineralogy and Petrology, Oxford University, for his very competent field and laboratory assistance during the summer and fall of 1967. Mr. Wicks carried out the X-ray analyses of the Muskox and Mount Albert specimens, and reported his findings, incorporated in this paper, in a thorough and competent way. Thanks are also due to the Management and Exploration Geology Staff of the Canadian Johns-Manville Co. Ltd., for free access to the Jeffrey Mine, and for permission to reproduce a simplified version of the geological and topographic map of the mine (Fig. 9). Similarly, thanks are due to Dr. B. D. Loncarevic for the permission and opportunity given to participate on the Bedford Institute of Oceanography Mid-Atlantic Ridge Geophysical cruise BI-22-68.

The photomicrographs of Figure 7 were taken by Mr. F. J. Cooke and the chemical analyses of Tables 7 and 8 were made by the Analytical Chemistry Section of the Geological Survey of Canada.

REFERENCES

Aruja, E.
1945: An X-ray study of the crystal structure of antigorite; *Mineral. Mag.*, vol. 27, pp. 65-74.

ASTM
1968: Standard diffraction pattern 7-239; American Society for Testing Materials, PDIS-18i.

Aumento, F.
1967: A serpentine mineral showing diverse strain-relief mechanisms; *Am. Mineralogist*, vol. 52, pp. 1399-1413.

1968: The Mid-Atlantic Ridge near 45°N. II. Basalts from the area of Confederation Peak; *Can. J. Earth Sci.*, vol. 5, pp. 1-21.

Bates, T.F.
1959: Morphology and crystal chemistry of 1:1 layer lattice silicates; *Am. Mineralogist*, vol. 44, pp. 78-114.

Bowen, N.L., and Tuttle, O.F.
1949: The system MgO-SiO_2-H_2O; *Geol. Soc. Am. Bull.*, vol. 60, pp. 439-460.

Brindley, G.W., and von Knorring, O.
1954: A new variety of Antigorite (Ortho-Antigorite) from Unst, Shetland Islands; *Am. Mineralogist*, vol. 39, pp. 794-804.

Brindley, G.W., and Zussman, J.
1959: Infra-red absorption data for serpentine minerals; *Am. Mineralogist*, vol. 44, pp. 185-188.

Brindley, G.W., Comer, J.J., Uyeda, R., and Zussman, J.
1958: Electron-optical observations with crystals of Antigorite; *Acta Cryst.*, vol. 11, pp. 99-102.

Busé, M.L., and Watson, E.H.
1960: Alteration of ultrabasic rocks near Bryn Mawr, Pennsylvania; *Penn. Acad. Sci. Proc.*, vol. 34, pp. 117-123.

Chapman, J.A., and Zussman, J.
1959: Further electron optical observations on crystals of Antigorite; *Acta Cryst.*, vol. 12, pp. 550-552.

Coleman, R.G.
1965: New Zealand serpentinites and associated metasomatic rocks; *New Zealand Geol. Surv.*, Bull. n.s. 76.

Epprecht, W., and Brandenburger, E.
1946: Die Entwasserung von Chrysotil und Antigorit; *Schweiz. Mineral Petr. Mitt.*, vol. 26, p. 229.

Findlay, D.C., and Smith, C.H.
1965: The Muskox Drilling Project; *Geol. Surv. Can.*, Paper 64-44.

Francis, G.H.
1956: The Serpentine mass in Glen Urquhart, Inverness-shire, Scotland; *Am. J. Sci.*, vol. 254, pp. 201-226.

Gillery, F.H.
1959: The X-ray study of synthetic Mg-Al serpentines and chlorites; *Am. Mineralogist*, vol. 44, pp. 143-152.

Hargreaves, A., and Taylor, W.H.
1946: An X-ray examination of decomposition products of chrysotile (asbestos) and serpentine; *Mineral. Mag.*, vol. 27, pp. 204-216.

Hess, H.H., Smith, R.J., and Dengo, G.
1952: Antigorite from the vicinity of Caracas, Venezuela; *Am. Mineralogist*, vol. 37, pp. 68-75.

Hess, H.H., and Otalora, G.
1964: Mineralogical and chemical composition of the Mayaguez serpentinite cores; NAS-NRC Publ. 1188, pp. 152-168.

Hey, M.H., and Bannister, F.A.
1948: A note on the thermal decomposition of chrysotile; *Mineral. Mag.*, vol. 28, pp. 333-337.

Hostetler, P.B., Coleman, R.G., Mumpton, F.A., and Evans, B.W.W.
1966: Brucite in Alpine serpentinites; *Am. Mineralogist*, vol. 51, pp. 75-98.

Huggins, C.W., and Shell, H.R.
1965: Density of bulk chrysotile and massive serpentine; *Am. Mineralogist*, vol. 50, pp. 1058-1067.

Irvine, T.N., and Smith, C.H.
1967: The ultramafic rocks of the Muskox Intrusion, Northwest Territories, Canada: *in* Ultramafic and related rocks, Editor: P.J. Wyllie; John Wiley & Sons, Inc., N.Y., pp. 38-49.

Kalousek, G.L., and Muttart, L.E.
1957: Studies on the chrysotile and antigorite components of serpentine; *Am. Mineralogist*, vol. 42, pp. 1-22.

Keen, C.E., and Barrett, D.L.
1969: Seismic structure on the Mid-Atlantic Ridge near 45°N; *Trans. Am. Geophys. Union*, vol. 50, p. 241.

Lapham, D.M.
1965: A new nickeliferous magnesium hydroxide from Lancaster County, Pennsylvania; *Am. Mineralogist*, vol. 50, pp. 1708-1716.

MacGregor, I.D.
1962: Geology, petrology, and geochemistry of the Mount Albert and associated ultramafic bodies of central Gaspé, Quebec; Unpubl. M.Sc. thesis, Queen's University.

Maser, M., Rice, R.V., and Klug, H.P.
1960: Chrysotile morphology; *Am. Mineralogist*, vol. 45, pp. 680-688.

Midgley, H.G.
1951: A serpentine mineral from Kennack Cove, Lizard, Cornwall; *Mineral. Mag.*, vol. 29, pp. 526-544.

Nagy, B.
1953: The structural pattern of serpentines; *Econ. Geol.*, vol. 48, pp. 591-597.

Nagy, B., and Faust, G.T.
1956: Serpentines: natural mixtures of chrysotile and antigorite; *Am. Mineralogist*, vol. 41, pp. 817-838.

Naumann, A.W., and Dresser, W.H.
1966: The influence of sample texture on chrysotile dehydroxylation; *Am. Mineralogist*, vol. 51, pp. 1200-1211.

Olsen, E.J.
1961: Six-layer ortho-hexagonal serpentine from the Labrador Trough; *Am. Mineralogist*, vol. 46, pp. 434-438.

1963: Equilibrium calculations in the system Mg, Fe, Si, O, H and Ni; *Am. J. Sci.*, vol. 261, pp. 943-956.

Raleigh, C.B.
1963: Fabrics of naturally and experimentally deformed olivine; Ph.D. Diss. California Univ., Los Angeles, Calif.

Roy, D.M., and Roy, R.
1954: An experimental study of the formation and properties of synthetic serpentines and related layer line silicates; *Am. Mineralogist*, vol. 39, pp. 957-975.

Rucklidge, J.C., and Zussman, J.
1965: The crystal structure of the serpentine mineral, lizardite. $Mg_3Si_2O_5(OH)_4$; *Acta Cryst.*, vol. 19, pp. 381-389.

Selfridge, G.C., Jr.
1936: An X-ray and optical investigation of the serpentine minerals; *Am. Mineralogist*, vol. 21, pp. 463-503.

Smith, C.H., and Kapp, H.E.
1963: The Muskox Intrusion, a recently discovered layered intrusion in the Coppermine River area, Northwest Territories, Canada; *Mineral Soc. Am.*, Spec. Paper 1, pp. 30-35.

Soboleff, N.D., and Tatarinoff, M.V.
1933: The cause of brittleness in chrysotile asbestos; *Econ. Geol.*, vol. 28, pp. 171-176.

Tilley, C.E.
1947: The dunite-mylonites of St. Paul's Rocks (Atlantic); *Am. J. Sci.*, vol. 245, pp. 483-491.

Turner, F., and Verhoogen, J.
1960: Igneous and metamorphic petrology; 2nd Edition; McGraw-Hill Book Co., New York.

Vermaas, F.H.S.
1953: The thermal characteristics of some Transvaal serpentines and the production of forsterite; *J. S. Africa Chem. Met. Mining Soc.*, vol. 53, p. 191.

Whittaker, E.J.W.
1956a: The structure of chrysotile II. Clinochrysotile; *Acta Cryst.*, vol. 9, pp. 855-862.

1956b: The structure of chrysotile III. Orthochrysotile; *Acta Cryst.*, vol. 9, pp. 862-864.

1956c: The structure of chrysotile IV. Parachrysotile; *Acta Cryst.*, vol. 9, pp. 865-867.

1956d: The study of chrysotile V. Diffuse reflexions and fibre textures; *Acta Cryst.*, vol. 10, pp. 149-155.

Whittaker, E.J.W., and Zussman, J.
1956: The characterization of serpentine minerals by X-ray diffraction; *Mineral. Mag.*, vol. 31, pp. 107-126.

Wicks, F.J., and Zussman, J.
1967: X-ray microbeam investigations of the nature of "α -serpentine", "γ -serpentine" and "Serpophite" (Abstract Only). Conf. Phys. and Chem. Asbestos Minerals; Oxford University.

Wolochow, D., and White, W.H.
1941: Thermal studies on asbestos; *Can. J. Res.*, vol. 19B, pp. 49-64.

Yada, K.
1967: Study of chrysotile asbestos by a high resolution electron microscope; *Acta Cryst.*, vol. 23, pp. 703-706.

Yoder, H.S., Jr.
1952: The MgO-Al_2O_3-SiO_2-H_2O system and the related metamorphic facies: *in Am. J. Sci.*, Bowen Volume; pp. 569-627.

Zussman, J.
1954: Investigation of the crystal structure of antigorite; *Mineral. Mag.*, vol. 30, pp. 498-512.

Zussman, J., and Brindley, G.W.
1957: Serpentines with 6-layer Ortho-Hexagonal cells; *Am. Mineralogist*, vol. 42, pp. 666-670.

Zussman, J., Brindley, G.W., and Comer, J.J.
1957: Electron diffraction studies of serpentine minerals; *Am. Mineralogist*, vol. 42, pp. 133-153.

APPENDIX

Table 1. Minerals detected in serpentine concentrate diffractograms from the Muskox Intrusion.

Sample No.	Rock Type	CHRYSOTILE	ANTIGORITE	LIZARDITE	BRUGNATELLITE	PYROAURITE	BRUCITE	CHLORITE	TALC	BIOTITE	OLIVINE	CLINOPYROXENE	ENSTATITE	TREMOLITE	MAGNETITE	CARBONATE
Layer 12.																
S-0066.9	Serp. Dunite			xx	x	x	tr.	x		x					x	
S-0128.5	Serp. Dunite			xx	x		x	tr.		x					tr.	
S-0207.8	Serp. Dunite			xx	x	x	tr.	x		x					x	
S-0324.5	Serp. Dunite			xx	tr.	x	x								x	
S-0403.3	Serp. Dunite			xx	x	x	x								x	
N-2564.3	Serp. Dunite			xx	tr.					x					x	
N-2584.8	Serp. Dunite			xx	x		x								x	
N-2603.9	Serp. Dunite			xx	tr.		x								x	
N-2934.1	Serp. Dunite			xx	tr.		x	x		tr.					x	
N-3034.5	Serp. Dunite			xx	x		x	x							x	
N-3175.6	Serp. Dunite			xx	x										x	
N-3184.8	Serp. Dunite			xx	tr.										x	
N-3222.4	Serp. Dunite			xx	tr.										x	
N-3266.5	Serp. Dunite			xx	tr.			tr.		tr.					x	
Layer 11.																
S-0510.9	Troctolitic Per.			xx							x	x				
Layer 10.																
S-0566.5	Troctolitic Per.			xx	x						tr.	tr.				
S-0579.8	Olivine Gabbro			xx							x				x	
Layer 8.																
S-0732.8	Olivine Clinopyroxenite			xx								x				
S-0760.5	Olivine Clinopyroxenite			xx	tr.							x				
Layer 7.																
S-0911.8	Serp. Dunite			xx	x		x								x	
S-1010.4	Serp. Dunite			xx	tr.			x		x					x	
Layer 6.																
S-1115.0	Olivine Clinopyroxenite			xx						tr.		x				
Layer 5.																
S-1204.5	Serp. Dunite			xx	tr.			x							x	
S-1306.0	Serp. Dunite			xx	tr.		tr.	x		x					x	
S-1405.9	Serp. Dunite			xx	x			x		x					x	
S-1520.2	Serp. Dunite			xx	x					x	x					
S-1601.8	Dunite (Transition Zone)			xx	x		tr.			x	tr.					
S-1642.7	Dunite (Transition Zone)			xx	x		tr.			tr.	x				x	
S-1703.3	Dunite			xx	x					x	x					
S-1743.2	Dunite			xx	x			tr.		x	x					

Note: serp. = serpentinized
per. = peridotite
xx = major concentrations
x = minor concentrations (< 5%)
tr. = trace concentrations (< 1%)

Table 2. Indexed Muskox lizardite diffractograms, giving computed least squares refined cell parameters.

	S 0207.8				S 0324.5		
hkℓ	d, Å Obs.	Calc.	I^1	I^2	d, Å Obs.	Calc.	I^3
002+	8.1		3	1	8.1		2
006[1]	7.8		10	12	7.8		11
001	7.3	7.317	100	100	7.3	7.314	100
001*					4.79		2
020	4.60	4.612	10	3	4.60	4.610	6
004+	4.07		3	1	4.06		<<1
021-0012[1]	3.90	3.901	5	4	3.90	3.900	4
002	3.655	3.658	51	42	3.658	3.657	42
200	2.652	2.657	3	2	2.663	2.659	2
024[1]	2.625		4	2	2.617		2
201	2.501	2.498	19	8	2.499	2.499	12
003	2.441	2.439	5	4	2.435	2.438	4
101*	2.368		4	1	2.357		1
040	2.340		3	1	2.330		1
202	2.151	2.150	7	2	2.148	2.151	4
004	1.828	1.829	5	1	1.826	1.829	1
203-102*	1.793	1.797	4	1	1.792	1.797	2
110*							
060	1.537	1.537	10	4	1.536	1.537	5
204	1.508	1.507	5	3	1.507	1.507	3
005	1.463	1.463	4	1	1.464	1.463	1
401	1.307	1.307	3	1	1.308	1.308	1
a		5.314	Å			5.319	Å
b		9.223				9.221	
c		7.317				7.314	

	S 0403.3			S 0566.5		
hkℓ	d, Å Obs.	Calc.	I^3	d, Å Obs.	Calc.	I^3
002+	8.1		1	8.1		2
006[1]	7.8		5			
001	7.3	7.311	100	7.3	7.309	100
001*	4.76		2			
020	4.61	4.615	5	4.61	4.617	5
004+	4.05		1	4.05		1
021-00.12[1]	3.92	3.902	2	3.90	3.904	1
002	3.655	3.655	40	3.657	3.655	47
200	2.658	2.662	1	2.659	2.662	2
024[1]	2.622		2			
201	2.498	2.501	9	2.501	2.501	11
003	2.435	2.437	4	2.439	2.436	4
101*	2.367		1			
040	2.337		1			
202	2.145	2.152	3	2.144	2.152	3
004	1.827	1.828	1	1.824	1.827	2
203-102*	1.795	1.797	2	1.795	1.797	2
110*						
060	1.538	1.538	4	1.539	1.539	5
204	1.506	1.506	3	1.506	1.507	4
005	1.462	1.462	1	1.462	1.462	1
401	1.310	1.309	1	1.310	1.309	1
a		5.323	Å		5.324	Å
b		9.230			9.234	
c		7.311			7.310	

Note: I^1 = intensities from concentrate and fluorite in epoxy resin
I^2 = intensities from concentrate on double-faced scotch tape
I^3 = intensities from concentrate and fluorite on double-faced scotch tape

Table 2 (Cont'd)

	S 0911.8				S 1010.4			
hkℓ	d, Å Obs.	Calc.	I^1	I^3	d, Å Obs.	Calc.	I^1	I^3
002+	8.1		5	2	8.1		2	1
006[1]								
001	7.3	7.312	100	100	7.3	7.316	100	100
001*	4.73		6	4				
020	4.63[B]	4.611	12	6	4.64[B]	4.609	10	6
004+	4.07		3	<<1				
021-0012[1]	3.92	3.900	4	1				
002	3.654	3.656	52	41	3.655	3.658	49	40
200	2.663	2.661	3	1	2.662	2.659	1	1
024[1]								
201	2.502	2.501	14	7	2.501	2.499	14	8
003	2.440	2.438	4	3	2.443	2.439	5	3
101*	2.369		2	<<1				
040	2.341		3	1	2.330		2	<1
202	2.153	2.152	5	2	2.151	2.151	5	2
004	1.826	1.828	3	1	1.829	1.829	2	1
203-102*	1.794	1.797	4	1	1.796	1.797	3	1
110*	1.579							
060	1.536	1.537	8	3	1.536	1.536	7	3
204	1.506	1.507	5	2	1.506	1.507	4	2
005	1.462	1.462	1	<1	1.463	1.463	2	<1
401	1.309	1.309	3	1	1.308	1.308	2	<<1
a		5.322	Å			5.318	Å	
b		9.222				9.218		
c		7.312				7.316		

	S 1204.5				S 1306.0			
hkℓ	d, Å Obs.	Calc.	I^1	I^2	d, Å Obs.	Calc.	I^1	I^2
002+	8.1		2	2	8.1		1	1
006[1]								
001	7.3	7.311	100	100	7.3	7.314	100	100
001								
020	4.65[B]	4.612	15	7	4.62	4.615	15	8
004+	4.07		3	1				
021-00.12[1]					3.91	3.903	6	1
002	3.655	3.657	53	42	3.652	3.657	52	42
200	2.667	2.666	3	1	2.646	2.662	3	1
024[1]								
201	2.501	2.505	18	6	2.500	2.501	19	7
003	2.441	2.437	5	3	2.440	2.438	5	4
101*								
040	2.334		4	1	2.339		5	3
202	2.149	2.154	6	1	2.147	2.152	5	2
004	1.830	1.828	2	1	1.830	1.828	3	1
203-102*	1.799	1.799	2	1	1.798	1.798	4	1
110*								
060	1.537	1.537	10	2	1.538	1.538	8	3
204	1.506	1.508	5	1	1.507	1.507	4	1
005	1.462	1.462		<1	1.462	1.463	3	1
401	1.312	1.312	1	<<1	1.310	1.310	3	<1
a		5.333	Å			5.324	Å	
b		9.224				9.230		
c		7.311				7.314		

* = brucite reflections
1 = pyroaurite reflections
\+ = brugnatellite reflections
Unmarked reflections are for lizardite

Table 3. Minerals detected in serpentine concentrate diffractograms from the Mount Albert Intrusion.

Sample No.	Rock Type	CHRYSOTILE	ANTIGORITE	LIZARDITE	BRUGNATELLITE	PYROAURITE	BRUCITE	CHLORITE	TALC	BIOTITE	OLIVINE	CLINOPYROXENE	ENSTATITE	TREMOLITE	MAGNETITE	CARBONATE
80% SERPENTINIZED																
SDM-8	Peridotite			xx	tr.		tr.				x		x	tr.		
SDM-260	"			xx	tr.		tr.	x								
SDM-265	"			xx			x	x	x		x			x		
SDM-265 B	"			xx	tr.		tr.	x	x		x			x		
SDM-628	"			xx	tr.		x				tr.		tr.			
SDM-628 A	"			xx			tr.				tr.		x			
60 - 80 % SERPENTINIZED																
SDM-17	Peridotite			xx	tr.		tr.				x		x	x		
SDM-41 A	"			xx	x		tr.				x		x	x		
SDM-43 A	"			xx	tr.	tr.	x									
SDM-44	"			xx	x		x				tr.					
SDM-45 B	"			xx	x		x		tr.		x					
SDM-47	"			xx	tr.		x				x					
SDM-50	"			xx	tr.		x		x		x		x	x		
SDM-52	"			xx	tr.		x		x		x		x	x		
SDM-59	"			xx	tr.		x				x		x	tr.		
SDM-60	"			xx			x				x		x			
SDM-105	"			xx	tr.		x				x					
SDM-118	"			xx	tr.		x				x		x	tr.		
SDM-126	"			xx	tr.		x				x		x			
SDM-190	"			xx	tr.		x	x	x		x		x	x		
SDM-207	"			xx			x	x			x		x	x		
SDM-228	"			xx	x		x	x	x		x		tr.	tr.		
SDM-570	"			xx	x		x				x		x			
SDM-642	"			xx				x	x		tr.			tr.		
40 - 60 % SERPENTINIZED																
SDM-150	Peridotite			xx	tr.		x				x		x			
SDM-168	"			xx	tr.		x	x	x		x			x		
SDM-267	"			xx	tr.			x	x					tr.		
SDM-268	"			xx	tr.		x				x					
20 - 40 % SERPENTINIZED																
SDM-607	Peridotite			xx				x			x		x	tr.		

Note: xx = major concentrations
x = minor concentrations (< 5%)
tr = trace concentrations (< 1%)

Table 4. Indexed Mount Albert lizardite diffractograms, giving computed least squares refined cell parameters.

	SDM-43 A			SDM-44			SDM-260			SDM-268			SDM-270			SDM-570			SDM-628		
	d, Å			d, Å			d, Å			d, Å			d, Å			d, Å			d, Å		
hkℓ	Obs.	Calc.	I	Obs.	Calc.	I	Obs.	Calc.	I	Obs.	Calc.	I	Obs.	Calc.	I	Obs.	Calc.	I	Obs.	Calc.	I
002+	8.1		1	8.1		1	8.1		1	8.1		1	8.1		1	8.1		1	8.1		1
006[1]	7.8		1										7.8		2						
001	7.3	7.311	100	7.3	7.312	100	7.3	7.305	100	7.3	7.295	100	7.3	7.308	100	7.3	7.302	100	7.3	7.306	100
001*	4.76		8	4.73[B]		3				4.76		8	4.71		3	4.75		3	4.75		6
020	4.62	4.617	6	4.62	4.620	3	4.60	4.611	7	4.61	4.612	3	4.62	4.612	6	4.61	4.624	3	4.61	4.609	6
004+	4.06		1	4.06		1	4.05		1	4.05		<1	4.06		1	4.05		1	4.05		1
021-00.12[1]	3.90	3.904	2	3.90	3.906	<1	3.90	3.900	1	3.90	3.898		3.90	3.900	1	3.89	3.907	1	3.90	3.898	1
002	3.657	3.656	45	3.658	3.656	41	3.650	3.653	47	3.653	3.651	41	3.653	3.654	42	3.652	3.651	40	3.652	3.653	41
200	2.663	2.662	1	2.669	2.668	<1	2.655	2.659	2	2.660	2.671	<1	2.652	2.660	2	2.664	2.667	1	2.660	2.660	2
201	2.503	2.501	11	2.503	2.507	5	2.498	2.498	14	2.501	2.508	4	2.499	2.499	10	2.505	2.505	6	2.499	2.499	8
003	2.438	2.437	4	2.439	2.437	2	2.438	2.435	5	2.440	2.435	2	2.440	2.436	4	2.437	2.434	3	2.437	2.436	4
101*	2.370		3	2.367		<1	2.367		<1	2.371		2	2.370		<1	2.358		<1	2.374		1
040	2.342		2	2.344		1	2.336		<<1				2.345		1						
202	2.154	2.152	4	2.154	2.155	2	2.146	2.149	4	2.156	2.156	2	2.152	2.151	3	2.155	2.154	2	2.149	2.150	2
004	1.827	1.828	1	1.828	1.828	1	1.826	1.826	1	1.827	1.826	1	1.828	1.827	1	1.827	1.827	1	1.827	1.827	1
203-102*	1.796	1.797	3	1.796	1.799	1	1.793	1.796	2	1.793	1.799	2	1.796	1.797	2	1.792	1.799	1	1.793	1.796	2
110*	1.577		1																		
060	1.539	1.539	5	1.540	1.540	2	1.537	1.537	6	1.537	1.537	2	1.537	1.537	4	1.541	1.541	3	1.536	1.536	4
204	1.507	1.507	3	1.507	1.508	1	1.504	1.505	3	1.507	1.507	1	1.504	1.506	3	1.507	1.506	2	1.506	1.506	2
005	1.462	1.462	1	1.463	1.462	<1	1.462	1.461	<1	1.461	1.461	1	1.462	1.462	1	1.460	1.460	<1	1.461	1.461	1
401	1.309	1.309	2	1.313	1.312	<1	1.308	1.308	1	1.315	1.314	1	1.309	1.309	1	1.312	1.312	<1	1.308	1.308	2
a	5.324 Å			5.336 Å			5.317 Å			5.343 Å			5.321 Å			5.333 Å			5.319 Å		
b	9.235			9.240			9.223			9.224			9.224			9.248			9.218		
c	7.312			7.312			7.305			7.305			7.308			7.302			7.306		

Note: I = intensities from concentrate and fluorite on double-faced scotch tape
* = brucite reflections + = brugnatellite reflections
1 = pyroaurite reflections Unmarked reflections are for lizardite

Table 5. Minerals detected in serpentine concentrate diffractograms from the Jeffrey Mine.

Sample No.	Rock Type	CHRYSOTILE	ANTIGORITE	LIZARDITE	BRUGNATELLITE	PYROAURITE	BRUCITE	CHLORITE	TALC	BIOTITE	OLIVINE	CLINOPYROXENE	ENSTATITE	TREMOLITE	MAGNETITE	CARBONATE
Zone # 1.	West Wall															
AG-67-2 A	Mt. br. Serp. Per.			xx			x									
AG-67-3	Dk. gr. Serp. Per. + Bst.	xx			tr.											
Zone # 2.	West Wall															
AG-67-4 A	Mt. lt. gr. Serp. Per. + XF.	x		xx	tr.		x				tr.					
AG-67-6 A	Mt. dk. gr. Serp. Per. + Bst.	x		xx	tr.											
Zone # 3.	West Wall															
AG-67-27 A	Mt. lt. gr. Serp. Per.	x		xx	x		x				tr.					
AG-67-28 B	Dk. grey altered Per. + Talc			xx			tr.	x	x							
AG-67-8 G	Mt. dk./lt. gr. Serp. + Bst.	x		xx	x											
AG-67-10 B	Mt. dk./lt. gr. Serp. Per. + MF.	x		xx	tr.		xx									
Zone # 4.	West Wall															
AG-67-12 D	Mt. dk. gr. Serp. Per.			xx												
AG-67-15 B	Banded dk./lt. gr. Serp. Per. + MF.	xx		xx	tr.											
AG-67-21 D	Mt. Serp. Per. + XF.	x		xx			x									
AG-67-23 A	Mt. Grey Serp. Per. + XF	x		xx	x		xx									
AG-67-17	Banded lt. gr. Serp. Per			xx			xx						x			
Zone # 4.	East Wall															
AG-67-55 B	Banded dk. gr. Serp. Per + Bst.			xx		tr.							tr.			
Zone # 5.	West Wall															
AG-67-16 B	Mt. dk. gr. Serp. Per. + Bst.			xx		tr.	x						tr.			
Zone # 5.	East Wall															
AG-67-40 C	Mt. gr./creamy white Serp. Per. + MF.	xx	x	x	tr.											
AG-67-43 B	Mt. gr./white Serp. Per. + XF.	xx		xx	tr.		xx									
AG-67-45 B	Mt. black/creamy white MF.			xx			xx				x					
AG-67-47 C	Dk. gr. Serp. Per. + MF + XF.	xx		x												
AG-67-49 A	Dk. gr./br. Serp. Per. + Bst.			xx				x								
AG-67-53 A	Dk. gr. Serp. Per. + Magnetite		x	xx	tr.			tr.							tr.	
Waste Zone.	South Wall															
AG-67-33 A	Banded dk. br. Mt. Serp. Per. + Bst.			xx												
AG-67-34 B	Mt. dk. gr. Serp. Per. + Bst.			xx												
AG-67-36 A	Mt. dk. gr. Serp. Per. + Bst.			xx												
AG-67-30 B	Mt. br. Serp. Per. + Bst.			xx	x		xx	x			tr.		tr.			

Note: serp. = serpentinized
mt. = mottled
XF = cross-fibre veins
br. = brown
gr. = green
xx = major concentrations
per. = peridotite
bst. = bastite
MF = mass fibre
dk. = dark
lt. = light
x = minor concentrations (< 5%)

tr. = trace concentrations (< 1%)

Table 6. Indexed Jeffrey Mine lizardite diffractograms, giving computed least squares refined cell parameters.

	AG 67 - 2a			AG 67 - 10b			AG 67 - 12d			AG 67 - 23a		
hkℓ	d, Å Obs.	Calc.	I	d, Å Obs.	Calc.	I	d, Å Obs.	Calc.	I	d, Å Obs.	Calc.	I
001	7.4	7.307	100	7.4	7.319	100	7.4	7.336	100	7.5	7.330	100
020	4.6	4.619	4	4.8	4.623	6	4.6	4.616	10	4.5	4.620	5
021	——	——	——	4.086	3.908	——	——	——	——	——	——	——
002	3.66	3.653	——	3.682	3.659	——	3.67	3.666	50	3.68	3.665	43
200	——	——	——	2.712	2.668	1	3.119	2.680	2	——	——	——
201	2.532	2.518	11	2.510	2.506	11	2.508	2.517	18	2.511	2.514	7
003	2.442	2.435	3	——	——	4	2.462	2.444	1	2.468	2.443	4
202	2.164	2.162	4	2.155	2.155	3	2.155	2.163	8	2.165	2.162	2
004	1.828	1.826	1	1.830	1.830	1	1.856	1.833	3	1.831	1.832	3
203	1.800	1.803	3	1.800	1.800	1	1.798	1.806	3	1.802	1.805	5
060	1.540	1.540	8	1.539	1.541	3	1.538	1.538	9	1.540	1.540	5
204	1.508	1.510	2	1.507	1.508	2	1.507	1.513	5	1.509	1.512	2
005	1.461	1.461	1	1.463	1.463	——	1.463	1.466	2	1.466	1.466	1
401	——	——	——	1.311	1.312	——	1.310	1.318	4	1.317	1.316	2
a		5.365			5.335			5.360			5.353	
b		9.237			9.246			9.229			9.241	
c		7.306			7.317			7.330			7.330	

	AG 67 - 28b			AG 67 - 30b			AG 67 - 33a		
hkℓ	d, Å Obs.	Calc.	I	d, Å Obs.	Calc.	I	d, Å Obs.	Calc.	I
001	7.3	7.329	100	7.2	7.285	100	7.4	7.328	100
020	4.6	4.611	5	4.6	4.596	5	4.65	4.620	9
021	3.92	3.903	1	3.87	3.887	1	3.924	3.908	1
002	3.682	3.664	30	3.620	3.643	42	3.680	3.663	37
200	2.660	2.663	1	2.642	2.655	1	——	——	——
201	2.575	2.503	7	2.486	2.495	10	2.513	2.505	14
003	2.489	2.443	8	2.423	2.429	6	2.465	2.442	1
202	2.160	2.154	1	2.140	2.146	5	2.160	2.155	8
004	1.834	1.832	2	1.817	1.822	2	1.832	1.832	2
203	1.797	1.800	2	1.788	1.792	1	1.800	1.801	3
060	1.537	1.537	6	1.532	1.532	5	1.540	1.540	8
204	1.511	1.509	3	1.501	1.502	2	1.506	1.509	5
005	1.463	1.466	2	1.461	1.457	1	1.465	1.465	1
401	1.309	1.310	1	1.308	1.306	2	1.311	1.311	3
a		5.325			5.311			5.331	
b		9.222			9.193			9.240	
c		7.328			7.287			7.327	

	AG 67 - 53a			AG 67 - 55b			AG 67 - 89		
hkℓ	d, Å Obs.	Calc.	I	d, Å Obs.	Calc.	I	d, Å Obs.	Calc.	I
001	7.2	7.275	100	7.5	7.360	100	7.5	7.327	100
020	4.5	4.595	5	4.6	4.618	6	4.6	4.616	5
021	3.86	3.885	1	——	——	——	3.94	3.905	1
002	3.606	3.638	42	4.200	3.678	——	3.694	3.663	53
200	2.638	2.657	1	2.675	2.660	1	2.670	2.661	1
201	2.485	2.496	10	2.514	2.501	11	2.517	2.501	6
003	2.415	2.425	6	2.463	2.452	4	2.454	2.442	9
202	2.140	2.146	5	2.158	2.155	3	2.157	2.153	2
004	1.815	1.819	2	1.832	1.840	1	1.835	1.832	1
203	1.789	1.791	41	1.800	1.803	1	1.801	1.800	1
060	1.532	1.532	5	1.539	1.539	3	1.538	1.538	3
204	1.506	1.501	2	1.508	1.513	2	1.508	1.509	1
005	1.456	1.455	1	——	——	——	1.463	1.465	1
401	1.307	1.307	2	——	——	——	1.308	1.309	1
a		5.314			5.319			5.322	
b		9.191			9.234			9.231	
c		7.277			7.356			7.326	

Note: I = intensities from concentrate and fluorite on double-faced scotch tape.

Table 7. Major element chemical analyses of Mid-Atlantic Ridge serpentinites.

	1	2	3	4	5	6	7	8	9	10	11	12
	6-1	6-5	108-3	112-1	165-1	165-2	165-8	182-1	192-1	192-3	156-10	159-10
SiO_2	37.90	38.13	37.14	37.70	37.91	37.15	36.48	35.39	38.11	37.83	37.81	31.22
TiO_2	0.06	0.04	0.06	0.03	0.09	0.09	0.14	0.11	0.10	0.08	0.12	0.17
Al_2O_3	2.22	2.06	2.84	3.92	0.69	2.97	5.57	2.14	1.50	0.86	2.23	1.20
Fe_2O_3	7.01	7.36	6.75	6.46	9.35	9.38	6.61	3.84	8.15	7.50	9.45	9.20
FeO	0.78	0.37	0.60	0.88	0.31	0.44	1.75	1.20	0.50	0.56	0.28	0.77
MnO	0.01	0.17	0.21	0.10	0.14	0.13	0.19	0.09	0.17	0.09	0.31	0.13
MgO	36.70	36.50	37.50	37.00	37.18	36.78	32.86	28.48	36.08	36.59	34.48	29.93
CaO	0.35	0.18	0.18	0.18	0.16	0.13	3.41	11.37	0.98	0.95	0.38	8.82
Na_2O	0.23	0.28	0.12	0.10	0.20	0.16	0.09	0.29	0.25	0.33	0.44	0.35
K_2O	0.03	0.20	0.01	0.00	0.04	0.04	0.04	0.06	0.04	0.07	0.04	0.02
H_2O	12.70	13.08	13.30	12.64	12.30	12.00	11.40	10.20	12.50	12.40	13.06	10.89
CO_2	0.4	0.1	0.2	0.1	0.2	0.1	<0.1	6.8	0.8	1.3	<0.1	6.1
P_2O_5	0.02	0.02	0.03	0.02	0.03	0.03	0.02	0.05	0.05	0.04	0.11	0.07
Cr_2O_3	0.47	0.32	0.32	0.29	0.34	0.41	0.89	0.22	0.34	0.31	0.35	1.08
NiO	0.25	0.18	0.22	0.21	0.12	0.11	0.12	0.11	0.14	0.12	0.21	1.31
Total	99.15	99.02	99.46	99.58	99.06	99.92	99.65	100.35	99.71	99.03	99.27	101.36

Note: Specimens 165-8, 182-1 and 159-10 contain organic carbonate contaminations.

Table 8. Trace element spectrographic analyses of Mid-Atlantic Ridge serpentines.

	1	2	3	4	5	6	7	8	9	10	11	12
	6-1	6-5	108-3	112-1	165-1	165-2	165-8	182-1	192-1	192-3	156-10	159-10
Sr	<20	n.f.	n.f.	n.f.	<20	<20	<20	1000	<20	<20	<20	1500
Ba	56	32	13	15	15	17	30	17	21	8	20	20
Cr	3200	2200	2200	2000	2300	2800	6100	1500	2300	2100	2420	7400
Zr	<30	<30	n.f.	n.f.	<30	<30	<30	35	<30	<30	<30	84
V	75	54	66	40	55	52	60	91	100	88	110	130
Ni	1900	1400	1700	1600	1000	860	960	910	1100	1000	1600	8800
Cu	100	130	93	130	140	120	100	80	32	24	190	45
Co	190	97	120	150	150	110	120	65	120	84	170	110
Sc	<10	<10	<10	<10	<10	<10	<10	<10	<10	<10	<10	<10

Note: n.f. = not found Specimens 165-8, 182-1 and 159-10 contain organic carbonate contaminations.

Table 9. Minerals detected in whole rock serpentine concentrate diffractograms from the Mid-Atlantic Ridge Intrusions.

Sample No. (AG-68-)	Rock Type	CHRYSOTILE	ANTIGORITE	LIZARDITE	BRUGNATELLITE	PYROAURITE	BRUCITE	CHLORITE	TALC	BIOTITE	OLIVINE	CLINOPYROXENE	ENSTATITE	TREMOLITE	MAGNETITE	CARBONATE
SERPENTINE SEAMOUNT:																
6-1 Serp. Conc.				xx									tr.			
6-1 Wh. Rock				xx				tr.					tr.		tr.	
6-5 Serp. Conc.				xx												
6-5 Wh. Rock				xx				tr.				tr.		tr.		x
6-7 Wh. Rock				xx				tr.					tr.			
165-1 Serp. Conc.				xx												
165-1 Wh. Rock				xx					tr.	tr.	tr.					
165-2 Serp. Conc.		x		xx												
165-2 Wh. Rock		x		xx							tr.					
165-8 Serp. Conc.				xx				x								
165-8 Wh. Rock				xx			tr.	x				tr.	tr.			
165-13 Wh. Rock				xx			tr.	tr.			tr.		tr.		tr.	
165-14 Wh. Rock				xx	tr.			tr.			tr.				x	
165-16 Wh. Rock				xx				tr.			tr.		tr.		x	
165-17 Wh. Rock				xx	tr.			x		tr.			tr.		x	
165-50 Wh. Rock Light				xx			tr.	x			tr.		tr.			
165-50 Wh. Rock Dark				xx	tr.			x		tr.	tr.		tr.		x	
OTHER OCCURRENCES AT 45°N:																
108-3 Serp. Conc.				xx												
108-3 Wh. Rock				xx							tr.					
112-1 Serp. Conc.				xx				tr.								
112-1 Wh. Rock				xx				x			tr.		tr.		tr.	
156-10 Serp. Conc.				xx					tr.							
156-10 Wh. Rock				xx										tr.		
159-10 Serp. Conc.		x		xx					tr.		tr.					
159-10 Wh. Rock		x		xx				tr.	tr.		tr.			x	x	x
182-1 Serp. Conc.				xx										tr.		
182-1 Wh. Rock				xx			tr.	x			tr.		tr.	x		x
192-1 Serp. Conc.			x	xx				x	x		tr.		tr.	tr.		
192-1 Wh. Rock			x	xx				x	x		tr.	tr.	x	tr.		
192-3 Serp. Conc.		x		xx				x	x							
192-3 Wh. Rock		x		xx				x	x		tr.		tr.			x
192-5 Wh. Rock				xx				tr.	x		tr.		tr.		tr.	

Note: serp. conc. = serpentine concentrate
wh. rock = whole rock "as is". xx = major concentrations
x = minor concentrations (>20% for chrysotile, >10% for antigorite, <5% for other minerals) tr. = trace concentrations (<1%)

Table 10. Indexed Mid-Atlantic Ridge lizardite diffractograms, giving computed least squares refined cell parameters.

	6-1			6-5			108-3			112-1			159-10		
hkℓ	d, Å Obs.	Calc.	I	d, Å Obs.	Calc.	I	d, Å Obs.	Calc.	I	d, Å Obs.	Calc.	I	d, Å Obs.	Calc.	I
001	7.3	7.304	100	7.3	7.301	100	7.3	7.302	100	7.3	7.286	100	7.3	7.302	100
020	4.59	4.603	6	4.59	4.602	3	4.58	4.609	4	4.59	4.605	6	4.59	4.603	6
021	3.90	3.894	2	3.91	3.893	1	3.89	3.898	1	3.89	3.892	2	3.90	3.894	1
002	3.645	3.652	41	3.649	3.651	40	3.639	3.651	42	3.645	3.643	45	3.645	3.651	42
200	2.657	2.656	1	2.656	2.653	1	2.663	2.667	1	2.653	2.663	1	2.656	2.651	1
201	2.496	2.496	11	2.497	2.494	5	2.501	2.505	7	2.494	2.501	6	2.497	2.497	14
003	2.437	2.435	4	2.440	2.434	3	2.434	2.434	4	2.433	2.429	2	2.435	2.434	4
202	2.144	2.148	4	2.146	2.146	2	2.152	2.153	3	2.145	2.150	2	2.146	2.149	4
004	1.825	1.826	1	1.824	1.825	1	1.823	1.826	1	1.822	1.822	1	1.827	1.826	1
203	1.794	1.795	4	1.790	1.793	2	1.791	1.798	3	1.794	1.795	3	1.794	1.795	4
060	1.534	1.534	6	1.534	1.534	3	1.537	1.536	4	1.535	1.535	4	1.535	1.534	6
204	1.504	1.505	3	1.505	1.504	3	1.511	1.506	3	1.503	1.503	2	1.503	1.505	3
005	1.462	1.461	1										1.461	1.461	1
401	1.307	1.307	2				1.312	1.312	1	1.311	1.310	1	1.308	1.307	1
a		5.312	Å		5.306	Å		5.333	Å		5.327	Å		5.315	Å
b		9.207			9.204			9.218			9.209			9.207	
c		7.304			7.301			7.302			7.286			7.302	

	165-1			165-2			165-8			182-1			192-1		
hkℓ	d, Å Obs.	Calc.	I	d, Å Obs.	Calc.	I	d, Å Obs.	Calc.	I	d, Å Obs.	Calc.	I	d, Å Obs.	Calc.	I
001	7.3	7.305	100	7.3	7.305	100	7.3	7.301	100	7.3	7.313	100	7.3	7.289	100
020	4.58	4.604	5	4.58	4.607	6	4.59	4.610	5	4.57	4.603	4	4.62	4.604	6
021	3.91	3.895	2	3.90	3.897	2	3.89	3.898	1				3.90	3.892	2
002	3.652	3.652	42	3.646	3.652	40	3.645	3.651	41	3.649	3.656	40	3.658	3.645	42
200	2.655	2.663	1	2.662	2.659	1	2.653	2.657	1	2.654	2.654	1	2.655	2.657	1
201	2.498	2.502	10	2.496	2.499	7	2.496	2.497	11	2.494	2.495	10	2.496	2.496	9
003	2.450	2.435	4	2.450	2.435	3	2.450	2.434	2	2.459	2.437	3	2.437	2.430	4
202	2.147	2.152	4	2.146	2.150	2	2.148	2.148	4	2.145	2.148	3	2.150	2.147	3
004	1.825	1.826	1	1.823	1.826	2	1.825	1.825	1	1.822	1.828	1	1.807	1.822	2
203	1.794	1.797	4	1.788	1.796	3	1.792	1.795	4	1.791	1.795	2	1.787	1.793	4
060	1.535	1.535	5	1.536	1.536	6	1.537	1.537	4	1.534	1.534	3	1.534	1.537	5
204	1.502	1.506	2	1.506	1.505	1	1.504	1.505	1	1.503	1.506	2	1.505	1.503	2
005	1.464	1.461	1	1.462	1.461	1	1.460	1.460	1	1.466	1.463	1	1.462	1.458	1
401	1.312	1.310	2	1.309	1.308	1	1.308	1.307	2	1.307	1.306	1	1.307	1.307	1
a		5.327	Å		5.318	Å		5.315	Å		5.308	Å		5.314	Å
b		9.208			9.215			9.220			9.206			9.208	
c		7.305			7.305			7.301			7.313			7.289	

Note: I = intensities from concentrate and fluorite on double-faced scotch tape.

Table 11. Averaged per cent impurity content for the different minerals phases in serpentine concentrates from the ultrabasic intrusives under investigation.

	Degree of Serpentinization	Olivine Composition (% Fo)	Lizardite	Brugnatellite	Brucite	Chlorite	Talc	Biotite	Olivine	Clinopyroxene	Enstatite	Tremolite	Magnetite
M.A.R.	>90%	81-87	92.6	0.2	0.2	2.0	1.0	0.2	0.6	0.2	0.8	0.7	1.5
MUSKOX	40-90	80-85	87.5	2.9	1.5	1.4		2.0	1.1	0.7			2.9
JEFFREY MINE	60-80		95.3	1.1	2.2	0.6	0.2		0.3		0.3		
MT. ALBERT	60-80	91-93	83.1	1.5	3.7	1.7	1.6		3.9		2.7	1.8	